Tanaka, K., Yoshimura, T., and Ichihara, A. (1989). Role of substrate in reversible activation of proteasomes (multi-protease complexes) by sodium dodecyl sulfate. J. Biochem. (Tokyo) *106*, 495–500.

Unno, M., Mizushima, T., Morimoto, Y., Tomisugi, Y., Tanaka, K., Yasuoka, N., and Tsukihara, T. (2002). The structure of the mammalian 20S proteasome at 2.75 Å resolution. Structure *10*, 609–618.

Witt, E., Zantopf, D., Schmidt, M., Kraft, R., Kloetzel, P.M., and Kruger, E. (2000). Characterisation of the newly identified human Ump1 homologue POMP and analysis of LMP7(β5i) incorporation into 20 S proteasomes. J. Mol. Biol. *301*, 1–9.

Molecular Biology of the Cell
Vol. 18, 569–580, February 2007

The Assembly Pathway of the 19S Regulatory Particle of the Yeast 26S Proteasome[D]

Erika Isono,*† Kiyoshi Nishihara,*‡ Yasushi Saeki,*§ Hideki Yashiroda,‖ Naoko Kamata,* Liying Ge,*¶ Takashi Ueda,* Yoshiko Kikuchi,* Keiji Tanaka,‖ Akihiko Nakano,*# and Akio Toh-e*§

*Department of Biological Sciences, Graduate School of Science, University of Tokyo, Tokyo 113-0033, Japan; †Entwicklungsgenetik, ZMBP, University of Tübingen, D-72076 Tübingen, Germany; ‖Tokyo Metropolitan Institute of Medical Science, Tokyo 113-8613, Japan; and #RIKEN Discovery Research Institute, Saitama 351-0198, Japan

Submitted July 26, 2006; Revised November 13, 2006; Accepted November 20, 2006
Monitoring Editor: William Tansey

The 26S proteasome consists of the 20S proteasome (core particle) and the 19S regulatory particle made of the base and lid substructures, and it is mainly localized in the nucleus in yeast. To examine how and where this huge enzyme complex is assembled, we performed biochemical and microscopic characterization of proteasomes produced in two lid mutants, *rpn5-1* and *rpn7-3*, and a base mutant Δ*N rpn2*, of the yeast *Saccharomyces cerevisiae*. We found that, although lid formation was abolished in *rpn5-1* mutant cells at the restrictive temperature, an apparently intact base was produced and localized in the nucleus. In contrast, in Δ*N rpn2* cells, a free lid was formed and localized in the nucleus even at the restrictive temperature. These results indicate that the modules of the 26S proteasome, namely, the core particle, base, and lid, can be formed and imported into the nucleus independently of each other. Based on these observations, we propose a model for the assembly process of the yeast 26S proteasome.

INTRODUCTION

The ubiquitin–proteasome system (UPS) is essential for the degradation of short-lived regulatory proteins that are involved in cell cycle regulation, DNA repair, signal transduction, apoptosis, and metabolic regulation as well as for the elimination of damaged or misfolded proteins (Hershko and Ciechanover, 1998; Schwartz and Ciechanover, 1999). The 26S proteasome acts at the final step of this pathway by degrading poly-ubiquitinated substrates, thereby ensuring the irreversibility of this pathway.

The 26S proteasome is a huge multicatalytic complex consisting of >30 different components that are divided into those of the 20S core particle (CP) and the 19S regulatory particle (RP). The RP can be biochemically further divided into two substructures, the base and the lid. The base consists of six AAA-ATPase subunits, *r*egulatory *p*article *t*riple-A ATPase (Rpt)1p–Rpt6p, and three non-ATPase subunits, *r*egulatory *p*article *n*on-ATPase (Rpn)1p, Rpn2p, and Rpn13p, whereas the lid is made of nine non-ATPases, Rpn3p, Rpn5p–Rpn9p, Rpn11p, Rpn12p, and Sem1p (Rpn15p) (Glickman *et al.*, 1998b; Leggett *et al.*, 2002; Funakoshi *et al.*, 2004; Sone *et al.*, 2004). Rpn10p, a non-ATPase subunit that binds polyubiquitin (Ub) chains (van Nocker *et al.*, 1996; Saeki *et al.*, 2002; Elsasser *et al.*, 2004), has been suggested to exist in the interface between the base and the lid (Fu *et al.*, 2001).

Interestingly, the composition of the lid is surprisingly similar to that of the COP9/signalosome and the eIF3, from which Glickman *et al.* (1998a) proposed that these protein complexes have diverged from a common ancestor. Most of the components of these complexes share a common proteasome/COP9/Initiation factor (PCI) domain, thought to serve as a scaffold for protein–protein interaction (Hofmann and Bucher, 1998), or a catalytic MPN+ domain (Maytal-Kivity *et al.*, 2002). Rpn11p (Verma *et al.*, 2002; Yao and Cohen, 2002; Guterman and Glickman, 2004) and CSN5 (Cope *et al.*, 2002), which are MPN+ domain proteins of the lid and the COP9, respectively, are the only known components to possess enzymatic activity in these complexes.

It was shown by immunoelectron microscopy (Wilkinson *et al.*, 1998) and by fluorescence microscopy of green fluorescent protein (GFP)-tagged proteasomes (Enenkel *et al.*, 1999) that in yeast, 26S proteasomes were mainly localized in the nucleus, especially on the inner nuclear membrane. Based on genetic data, the involvement of importin α/β in

This article was published online ahead of print in *MBC in Press* (http://www.molbiolcell.org/cgi/doi/10.1091/mbc.E06-07-0635) on November 29, 2006.

[D] The online version of this article contains supplemental material at *MBC Online* (http://www.molbiolcell.org).

Present addresses: ‡ Graduate School of Frontier Sciences, University of Tokyo, Chiba 277-8561, Japan; § Tokyo Metropolitan Institute of Medical Sciences, Tokyo 113-8613, Japan; ¶ Graduate School of Frontier Sciences, University of Tokyo, Tokyo 108-8639, Japan.

Address correspondence to: Akio Toh-e (toh-e@rinshoken.or.jp).

Abbreviations used: CBB, Coomassie brilliant blue; CP, core particle; FRAP, fluorescence recovery after photobleaching; GFP, green fluorescent protein; MCA, methycoumaryl-7-amide; NLS, nuclear localization signal; PCI, proteasome/COP9/Initiation factor; mRFP, monomeric red fluorescent protein; RP, regulatory particle; Rpn, regulatory particle non-ATPase; Rpt, regulatory particle triple A ATPase; Suc-LLVY, succinyl-leucyl-leucyl-valyl-tyrosyl; Ub, ubiquitin; UFD, ubiquitin fusion degradation; UPS, ubiquitin–proteasome system.

Table 1. Yeast strains used in this study

Strain	Relevant genotype	Source
W303-1A	MATa *leu2 trp1 his3 ura3 ssd1 can1 ade2*	Our stock
W303-1B	MATα *leu2 trp1 his3 ura3 ssd1 can1 ade2*	Our stock
YEK5	MATa *rpn7::rpn7-3-URA3*	Isono *et al.* (2004)
YEK6	MATα *rpn7::rpn7-3-URA3*	Isono *et al.* (2004)
YEK29	YEK5 *rpn11::RPN11-3×FLAG-HIS3*	Isono *et al.* (2004)
YEK79	MATα *pre6::PRE6-GFP-TRP1*	This study
YEK100	MATa *rpn5::rpn5-1-TRP1*	This study
YEK101	MATα *rpn5::rpn5-1-TRP1*	This study
YEK115	MATa *rpn11::RPN11-YGFP-TRP1*	This study
YEK147	MATa *rpn1::RPN1-YGFP-LEU2*	This study
YEK209	YEK5 *rpn11::RPN11-YGFP-TRP1*	This study
YEK211	YEK5 *pre6::PRE6-YGFP-LEU2*	This study
YEK213	YEK6 *rpn1::RPN1-YGFP-LEU2*	This study
YEK221	MATα *rpn7::RPN7-3×FLAG-KanMX*	This study
YEK225	YEK100 *rpn7::RPN7-3×FLAG-KanMX*	This study
YEK234	YAT2433 *rpn1::RPN1-3×FLAG-HIS3*	This study
YEK235	YAT2433 *rpn1::RPN1-YGFP-LEU2*	This study
YEK236	YAT2433 *rpn11::RPN11-YGFP-TRP1*	This study
YEK246	YAT2433 *srp1::srp1-49-LEU2*	This study
YEK247	YAT2433 *srp1::srp1-49-LEU2 rpn7::RPN7-YGFP-URA3*	This study
YEK248	YAT2433 *srp1::srp1-49-LEU2 rpn1::RPN1-YGFP-URA3*	This study
YKN6	YEK100 *pre1::PRE1-3×FLAG-HIS3*	This study
YKN8	YEK100 *rpn1::RPN1-3×FLAG-HIS3*	This study
YKN16	YEK100 *rpn1::RPN1-YGFP-LEU2*	This study
YKN18	YEK101 *pre6::PRE6-YGFP-TRP1*	This study
YAT2433	MATα Δ*rpn2-TRP1* [Top2612]	This study
YAT3507	YAT2433 *rpn11::RPN11-3×FLAG-LEU2*	This study
YYS37	MATa *pre1::PRE1-3×FLAG-HIS3*	Saeki *et al.* (2002)
YYS39	MATa *rpn1::RPN1-3×FLAG-HIS3*	Saeki *et al.* (2002)
YYS40	MATa *rpn11::RPN11-3×FLAG-HIS3*	Saeki *et al.* (2002)

All strains are in the W303 background.

the nuclear import of the proteasomes was suggested (Tabb *et al.*, 2000), and it was shown that in the mutant of importin α *srp1-49*, seclusion of GFP-fused proteasome in the nucleus was no longer observed (Wendler *et al.*, 2004). A study in fission yeast has shown that Cut8 is responsible for retaining the proteasome within the nucleus (Tatebe and Yanagida, 2000; Takeda and Yanagida, 2005).

The process of proteasome assembly has been a topic for recent studies and interesting facts have been elucidated. The CP, which is a stack of four seven-membered rings, in the order of α7β7β7α7, is imported into the nucleus as an α7β7 "half" proteasome (Chen and Hochstrasser, 1996; Ramos *et al.*, 1998), and maturation is thought to take place in the nucleus (Fehlker *et al.*, 2003). Ump1p, which associates specifically with half-proteasomes, is suggested to function as an accelerator in this process (Ramos *et al.*, 1998). Blm10p (formerly registered as Blm3p) was reported to act as an inhibitor of premature dimerization of the half-proteasomes (Fehlker *et al.*, 2003), but it is also suggested to be a functional homologue of the mammalian PA200, activator of the CP (Schmidt *et al.*, 2005). Recently, a study in mammalian cells showed that PAC1 and PAC2 work during the first step of assembly of the α ring (Hirano *et al.*, 2005).

For the assembly of the RP, no external factors are known to date. In previous studies, we have shown that partially assembled lid subcomplexes made up of five (lid$^{rpn7\text{-}3}$: Rpn5p, Rpn6p, Rpn8p, Rpn9p, and Rpn11p) or four (lid$^{rpn6\text{-}1}$: Rpn5p, Rpn8p, Rpn9p, and Rpn11p) components accumulate in lid mutants (Isono *et al.*, 2004, 2005). Because Rpn5p, Rpn8p, Rpn9p, and Rpn11p were included in both subcomplexes, we proposed these to be the "core" of lid formation. In this study, based on the analysis of an *rpn5* mutant and an *rpn2* mutant, we show, for the first time, that the formation and nuclear import of both the lid and the base are separable processes and that Rpn5p is indeed one of the core components of the lid.

MATERIALS AND METHODS

Strains, Media, and Genetic Methods

Yeast strains used in this work are listed in Table 1, and plasmids used for cloning and subcloning various genes and their fragments are listed in Table 2. Cells were cultured in omission medium prepared by removing appropriate nutrient(s) from synthetic complete (SC) medium, rich medium (YPDAU) (Sherman *et al.*, 1986), or SR-U in which 2% glucose of SC was replaced with 2% raffinose and uracil was omitted. *Escherichia coli* strain DH5α (*supE44 ΔlacU169* [*ϕ80lacZ ΔM15*] *hsdR17 recA1 endA1 gyrA96 thi-1 relA1*) was used for construction and propagation of plasmids. Yeast transformations were performed as described previously (Burk *et al.*, 2000).

Isolation of Temperature-sensitive Mutants

Temperature-sensitive *rpn5* mutants were screened as described previously (Isono *et al.*, 2005). The *RPN5* gene was amplified using primers Rpn5 Mut1 (BglII) 5′-GGCCAAGATTGTAGATCTGCTAGC-3′ and Rpn5 Mut2 (NotI) 5′-GGAAGCGGCCGCAACCAGGCTTGAGTTAAC-3′ and cloned between the BamHI–NotI sites of the YIp vector pRS304. The resulting plasmid pNS101 was used as a template for polymerase chain reaction (PCR) mutagenesis.

Gel Filtration

Total proteins (5 mg) were resolved on a Superose 6 column (GE Healthcare, Little Chalfont, Buckinghamshire, United Kingdom) as described previously (Isono *et al.*, 2005). For the subsequent fractionation of Superose 6-fractionated samples, 450 μl of the separated samples were applied onto a Superdex 200 gel filtration column (GE Healthcare) connected to a fast-performance liquid

Table 2. Plasmids used in this study

Plasmid	Characteristics	Source
pRS304	*TRP1 Amp*^{r}	Sikorski and Hieter (1989)
pRS313	*HIS3 CEN Amp*^{r}	Sikorski and Hieter (1989)
Ub-A-lacZ	*GAL1p-Ub-A-lacZ URA3 Amp*^{r}	Bachmair *et al.* (1986)
Ub-R-LacZ	*GAL1p-Ub-R-lacZ URA3 Amp*^{r}	Bachmair *et al.* (1986)
Ub-P-lacZ	*GAL1p-Ub-P-lacZ URA3 Amp*^{r}	Bachmair *et al.* (1986)
pTS901CL	*5×HA CEN LEU2 Amp*^{r}	Sasaki *et al.* (2000)
pEK152	*RPN11-YGFP-TRP1 Amp*^{r}	This study
pEK165	*PRE6-YGFP-TRP1 Amp*^{r}	This study
pEK221	*RPN5(−400bp ORF∼+1kb ORF) HIS3 CEN Amp*^{r}	This study
pEK252	*RPN1-YGFP-LEU2 Amp*^{r}	This study
pEK285	*NUP53-mRFP-LEU2 CEN Amp*^{r}	This study
pEK291	*RPN7-YGFP-URA3 Amp*^{r}	This study
pEK296	*RPN1-YGFP-URA3 Amp*^{r}	This study
pEK297	*RPN3-YGFP-URA3 CEN Amp*^{r}	This study
pEK298	*RPN7-YGFP-URA3 CEN Amp*^{r}	This study
pEK299	*RPN12-YGFP-URA3 CEN Amp*^{r}	This study
pEK300	*RPN15-YGFP-URA3 CEN Amp*^{r}	This study
pNS101	*RPN5 TRP1 Amp*^{r}	This study
pNS202	*GST-RPN5 Amp*^{r}	This study
TOp2612	*ΔN rpn2 (+437∼+2838) HIS3 CEN Amp*^{r}	This study

chromatograph (GE Healthcare) at a flow rate of 0.5 ml/min, and 500-μl serial fractions were collected using a fraction collector FRAC-100 (GE Healthcare).

Microscopy

Cells harboring GFP- or monomeric red fluorescent protein (mRFP)-fused proteins were photographed by using a BX52 fluorescence microscope (Olympus, Tokyo, Japan) with a UPlanApo 100×/1.45 objective (Olympus) equipped with a confocal scanner unit CSU20 (Yokogawa Electric, Tokyo, Japan) and an EMCCD camera (Hamamatsu Photonics, Bridgewater, NJ). GFP and mRFP were excited using the 488- and 568-nm Ar/Kr laser lines with GFP and RFP filters (Semrock, Rochester, NY), respectively. DNA stained with Hoechst 33342 was photographed using a 405-nm laser line with a UV filter (Semrock). Images were obtained and processed using the IPLab software (Scanalytics, Fairfax, VA) and processed using Photoshop 7.0 (Adobe Systems, Mountain View, CA). For DNA staining, a final concentration of 20 μg/ml Hoechst 33342 (Sigma-Aldrich, St. Louis, MO) was added to the cell suspension and incubated for 10 min at either 25 or 37°C under a light shade.

Fluorescence Recovery after Photobleaching (FRAP)

Samples used for FRAP experiments were embedded in agarose in the following way with modifications of the methods described previously (Hoepfner *et al.*, 2000). First, 100 μl of 1.7% agarose (Takara, Kyoto, Japan) dissolved in filtrated SC media was dropped on a prewarmed holed glass slide (Toshinriko, Tokyo, Japan), and immediately covered with a coverslip (Matsunami Glass, Osaka, Japan). Excess agarose was removed, and the glass slide was cooled until the agarose was set. The coverslip was carefully removed, and 3 μl of freshly cultured cells was dropped on the agarose plane and covered with a new coverslip and sealed. FRAP experiments were performed using a confocal laser-scanning microscope LSM510 META (Carl Zeiss, Jena, Germany) with a Plan-APOCHROMAT 100×/1.4 objective (Carl Zeiss). GFP was excited using the 488-nm laser lines from an Ar ion laser and a GFP filter. Photobleaching was achieved by scanning the selected region with maximal output of the 488-nm laser, and the recovery of the fluorescent signal was observed at the indicated time points under the same recording conditions as at 0 min. The stage was kept at 37°C with a stage-heater MATS-525F (Tokai Hit, Shizuoka, Japan). Fluorescence intensity of the original data was quantified using the LSM510 software, and images were processed with Photoshop 7.0 (Adobe Systems).

Indirect Immunofluorescence Method

For fixation, 420 μl of 37% formaldehyde was added to 3 ml of logarithmically growing cell culture (OD_{600} = 0.8–1.0) and incubated for 30 min at the incubation temperature. Cells were centrifuged and resuspended in 500 μl of phosphate-buffered saline (PBS)-formaldehyde (PBS/formaldehyde, 10:1) and incubated for 30 min at room temperature. For spheroplasting, cells were incubated with 200 μl of PBS-zymolyase (20 μg of zymolyase 100T [Seikagaku America, Rockville, MD]/1 ml of PBS) for 20 min at 30°C. Cells were then incubated in 200 μl of PBS containing 0.5% Triton X-100 for 30 min at room temperature. After washing twice, cells were resuspended in 200 μl of 3% bovine serum albumin in PBS for blocking and incubated for 1 h at room temperature. Mouse monoclonal anti-FLAG M2 antibody (Sigma-Aldrich, St. Louis, MO; 1/200 dilution) or anti-Rpn5p (1/100 dilution) antibody was used as primary antibody. Alexa Fluor 488 goat anti-mouse IgG (Molecular Probes, 1/400 dilution) or Alexa Fluor 546 goat anti-rabbit IgG (1/400 dilution; Invitrogen, Carlsbad, CA) was used as a secondary antibody. DNA was stained with 0.5 μg/ml 4,6-diamidino-2-phenylindole (DAPI) (Sigma-Aldrich).

RESULTS

Isolation of the Temperature-sensitive rpn5-1 Mutant

In our previous study, we found that partially assembled lid subcomplexes accumulated in temperature-sensitive lid mutants. Five (Rpn5p, Rpn6p, Rpn8p, Rpn9p, and Rpn11p) or four (Rpn5p, Rpn8p, Rpn9p, and Rpn11p) out of the nine components of the lid formed a stable complex in lid mutants, *rpn7-3* (Isono *et al.*, 2004) and *rpn6-1/rpn6-2* (Isono *et al.*, 2005), respectively. From these results and the fact that *RPN9* is a nonessential gene, we hypothesized that Rpn5p, Rpn8p, and Rpn11p may play pivotal roles in producing the core of the lid. To examine this hypothesis, we first focused on the function of Rpn5p.

To start with, we generated a temperature-sensitive mutant allele of *RPN5* by PCR-based random mutagenesis (Cadwell and Joyce, 1992; Toh-e and Oguchi, 2000) and named it *rpn5-1*. The *rpn5-1* mutant grew normally at 25°C, but it stopped growth after 6–8 h at 37°C (data not shown). The growth defect of the *rpn5-1* mutant at 37°C was complemented by a single copy of the wild-type *RPN5* gene, proving that the temperature sensitivity is due to a mutation within the *RPN5* gene and that the *rpn5-1* mutation is not dominant (Figure 1A). Sequencing analysis revealed that the *rpn5-1* open reading frame (ORF) possessed three mutations (Figure 1B), of which I180L or R344G alone did not lead to temperature-sensitive growth when introduced into the wild-type background. The nucleotide substitution from G to A at the 1245th nucleotide, leading to a nonsense mutation at the 415th tryptophan was found to be responsible for the temperature sensitivity (data not shown). Amounts of Rpn5-1p along with other proteasomal components were not significantly changed during incubation at the restrictive temperature, whereas a slight mobility shift of Rpn5-1p was

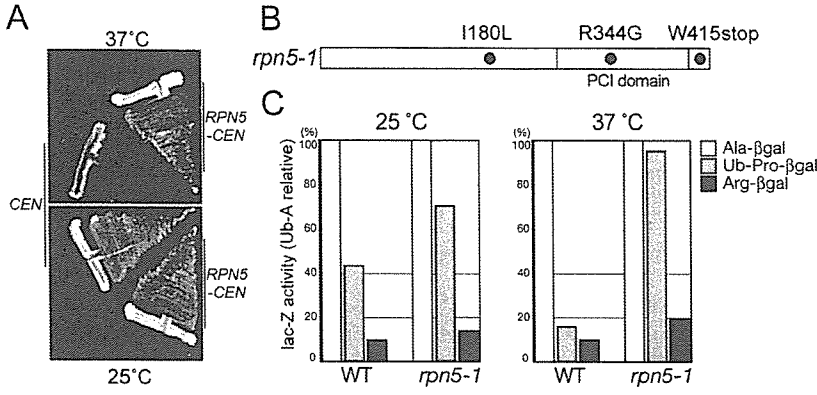

Figure 1. Characterization of the temperature-sensitive *rpn5* mutant. (A) *rpn5-1* (YEK100) cells carrying either a *CEN* vector (pRS314) or *RPN5-CEN* plasmid (pEK221) were streaked on YPDAU plates and photographed after incubating for 2 d at either 25 or 37°C. (B) Amino acid substitution in *rpn5-1*. The nucleotide sequence of the *rpn5-1* ORF was determined by the dideoxychain termination method and compared with that of the wild-type *RPN5* ORF. Gray, PCI domain. (C) Degradation of N-end rule pathway- and UFD pathway-substrates. Wild-type (W303-1A) and *rpn5-1* (YEK100) cells were transformed with plasmids expressing an N-end rule model substrate Ub-Ala-βgal or Ub-Arg-βgal, or a UFD pathway substrate Ub-Pro-βgal. Production of the model substrates was induced by adding 2% galactose to SR-U medium. Cells were harvested after 4 h of induction at either 25 or 37°C, and steady-state levels of β-galactosidase activity were assayed. The amounts of Ub-Pro-βgal and Arg-βgal are indicated relative to that of Ala-βgal. Average of three independent experiments is shown (open, Ala-βgal; light gray, Ub-Pro-βgal; and solid, Arg-βgal).

observed due to the C-terminal truncation (Supplemental Figure 1).

To examine the effect of the *rpn5-1* mutation on the UPS, we evaluated the stability of three model substrates of the ubiquitin–proteasome pathway, namely, Ala-βgal, Arg-βgal, and Ub-Pro-βgal (Bachmair *et al.*, 1986). Whereas Ala-βgal is stable, Arg-βgal, and Ub-Pro-βgal are short-lived substrates of the N-end rule- and Ub-fusion degradation (UFD) pathway, respectively. Wild-type and *rpn5-1* mutant cells, transformed with plasmids expressing one of these substrates under a galactose inducible promoter were cultured at either 25 or 37°C. After 3 h, galactose was added to the culture to induce the production of the substrates, and cells were incubated for further 4 h. Total extract was prepared from each culture, and steady-state levels of the substrates were estimated by β-galactosidase assay. Compared with the wild-type cells, *rpn5-1* cells maintained the normally short-lived Arg-βgal and Ub-Pro-βgal at a higher level, especially at 37°C, indicating that the *rpn5-1* mutation caused a defect in the UPS at the restrictive temperature (Figure 1C).

Assembly of the Lid in rpn5-1 Mutants

In a previous report on a Δ*rpn5* mutant in fission yeast, the state of assembly of each substructure of the 26S proteasome was ambiguous, because Rpn10p that is not stably associated with the base or the lid was used for the affinity purification of proteasomes (Yen *et al.*, 2003a). To examine the assembly of the 26S proteasome in the *rpn5-1* mutant, we compared the gel filtration profile of proteasomes in wild-type and *rpn5-1* extracts. Wild-type and *rpn5-1* cells were cultured for 7 h at 37°C in YPDAU, and total lysates were prepared in the presence of ATP and $MgCl_2$. Extract equivalent to 5 mg of protein was resolved on a Superose 6 gel filtration column, and the eluate was collected into 500 μl of sequential fractions. Relevant fractions (16~32) were subjected to peptidase activity measurement by using succinyl-leucyl-leucyl-valyl-tyrosyl-methycoumaryl-7-amide (Suc-LLVY-MCA), a fluorogenic peptide substrate. In the wild-type sample, the most enzymatically active fraction was at 22, showing this fraction to be the peak fraction of the 26S holoenzyme (Figure 2A, top).

In contrast, in gel filtration of extract prepared from 37°C-grown *rpn5-1* cells, the peak at fraction 22 has almost vanished, suggesting that the assembly of the 26S proteasome is disturbed. On SDS treatment, which activates free CPs, a high enzyme activity occurred at fractions 26 and 27, indicating that there is a large pool of free CPs in *rpn5-1* cells grown at 37°C (Figure 2A, bottom). There was also a small peak in fraction 23, the identity of which will be discussed later. *rpn5-1* cells cultured at 25°C had almost the same profile as the wild-type, except that the peak of enzyme activity at fraction 26 was higher than that in the wild-type sample (Figure 2A, middle).

Fractions were then subjected to Western blotting by using antibodies against proteasome components. CP signals were detected around fraction 22 in the wild type sample, whereas they were detected around fraction 26 in the sample derived from *rpn5-1* cells grown at 37°C, in accordance with the result of activity measurement (Figure 2B, top and bottom). Interestingly, all lid components of *rpn5-1* cells grown at 37°C, but not at 25°C, were detected in low-molecular-mass fractions (Figure 2B, middle and bottom). To investigate whether they are monomers or forming a complex, we further resolved fractions 32 and 34 by Superdex 200, and fractions were subjected to Western blotting (Figure 2C). Comparison with marker proteins indicated that at least Rpn5p (52 kDa), Rpn8p (38 kDa), and Rpn9p (46 kDa) existed in a free form. Rpn7p (49 kDa) was found to move slower than expected from its molecular mass.

To see whether Rpn7p forms a stable complex with any other components in *rpn5-1* cells, we generated *rpn7::RPN7-3xFLAG* strains with or without the *rpn5-1* mutation and performed affinity purification. *RPN7-3xFLAG RPN5* and *RPN7-3xFLAG rpn5-1* strains were cultured at either 25 or 37°C for 7 h and proteasomes were affinity purified by anti-FLAG antibody immobilized on agarose from total lysates. Purified proteasomes were resolved by SDS-PAGE and stained with Coomassie brilliant blue (CBB), and the band patterns were compared with purified authentic proteasomes (Saeki *et al.*, 2005). All components of the 26S proteasome were copurified with Rpn7p-3xFLAG in wild-type cells and *rpn5-1* cells cultured at 25°C (Figure 2D, lanes 2 and 3; data for wild-type 25°C not shown). However, no protein was copurified with Rpn7p-3xFlag from *rpn5-1* cells cultured at 37°C. Because Rpn7p-3xFLAG was present in the total extract at both 37 and 25°C (Supplemental Figure 2), Rpn7p is probably not forming a soluble and stable complex with other components in *rpn5-1* cells under the restrictive conditions.

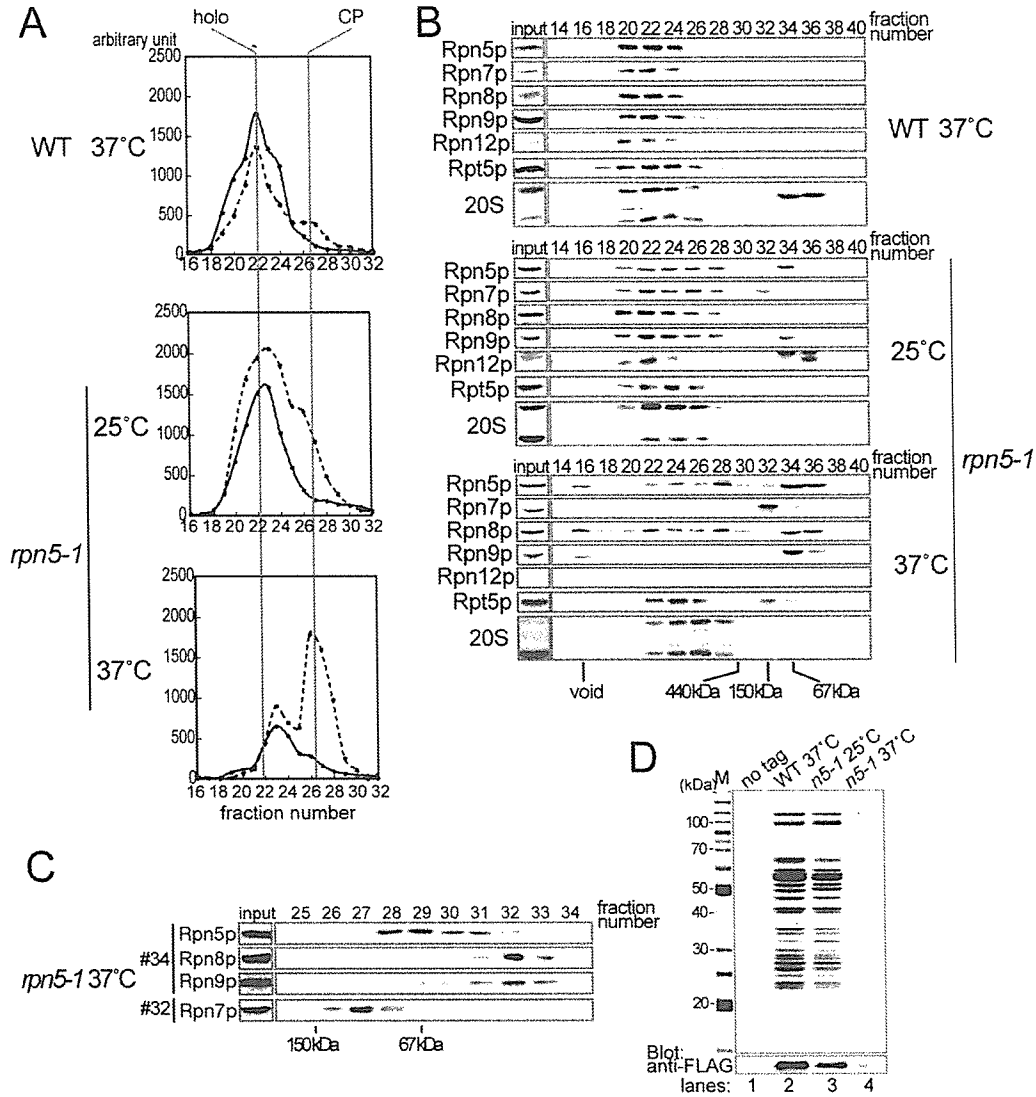

Figure 2. Lid formation in *rpn5-1* cells. Wild-type (W303-1A) and *rpn5-1* (YEK100) cells were cultured for 7 h at the indicated temperature, and total cell extracts were prepared by breaking the cells by glass-beads under the existence of ATP and $MgCl_2$. (A) Gel filtration. Peptidase activity toward the fluorogenic substrate Suc-LLVY-MCA was measured in relevant fractions (16–32). Positions of the 26S holoenzyme and the CP are indicated at the top of the graph. Solid line, without SDS; and dotted line, with 0.02% SDS. (B) Western blotting. Twenty microliters of each of the even numbered fractions was mixed with SDS-PAGE loading buffer and resolved by 12.5% SDS-PAGE, transferred to polyvinylidene difluoride membrane, and proteasome subunits were detected by Western blotting by using the indicated antibodies (Rpn5p, Rpn7p, Rpn8p, Rpn9p, and Rpn12p, lid; and Rpt5p, base) Positions of the void fraction and marker proteins (ferritin [440 kDa], aldolase [150 kDa], and bovine serum albumin [67 kDa]) are indicated at the bottom of the panels. (C) Second gel filtration. Fractions 32 and 34 in Superose 6 gel filtration of *rpn5-1* extracts (37°C) in A were subsequently resolved by a Superdex 200 gel filtration column. Five hundred microliters sequential fractions were collected, and relevant fractions were subjected to Western blotting as in B. Antibodies used are indicated on the left. Positions of marker proteins (aldolase [150 kDa] and bovine serum albumin [67 kDa]) are indicated on the bottom of the panels. (D) Wild-type and *rpn5-1* strains expressing *RPN7-3xFLAG* (YEK221 and YEK225, respectively) along with the untagged wild-type strain (W303-1A) were cultured for 7 h at 25 or 37°C as indicated, and extract was prepared from each culture. Proteasomes were affinity purified using anti-FLAG agarose. Purified products were run on a 12.5% SDS-PAGE gel, and protein bands were stained with CBB (M, marker).

Base-CP Complexes in rpn5-1

The base and the CP of the extract prepared from *rpn5-1* cells incubated at 37°C seemed to comigrate (Figure 2B). Results of nondenaturing PAGE of total lysates of wild-type or *rpn5-1* cells grown at 37°C showed the existence of base-CP complexes, B1CP, and B2CP, in *rpn5-1* cells (Figure 3A). The peak of peptidase activity observed in fraction 23 in the *rpn5-1* sample grown at 37°C (Figure 2A, bottom) was likely due to these base–CP complexes. We next tried to affinity-purify these base–CP complexes by using CP- or base-tagged strains. However, as shown in Figure 3B, no base–CP complex was obtained from *rpn5-1* cells regardless of the tagged subunit used, suggesting that the base-CP interaction in *rpn5-1* cells is unstable.

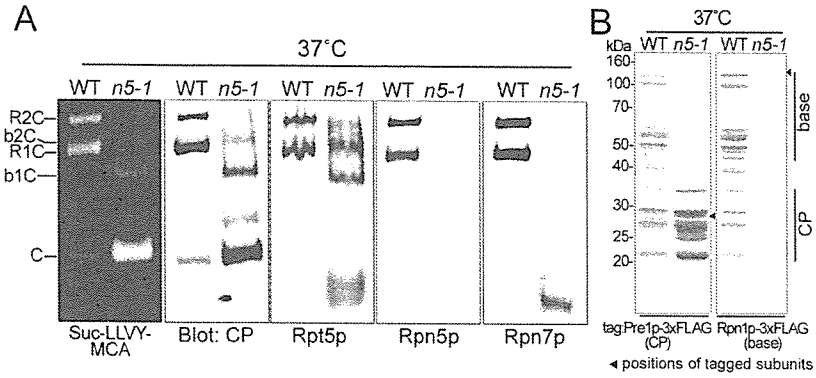

Figure 3. Proteasome species in wild-type extract and *rpn5-1* extract. (A) Extracts were prepared from wild-type (W303-1B) or *rpn5-1* (YEK101) cells incubated for 7 h at 37°C, and extract equivalent to 50 μg of protein was resolved by nondenaturing PAGE. Proteasomes were visualized by overlaying buffer containing 0.1 mM Suc-LLVY-MCA and 0.05% SDS on the gel (far left). The gels were subsequently subjected to Western blotting by using antibodies indicated on the bottom of the panels (Rpt5p, base; and Rpn5p and Rpn7p, lid). Bands corresponding to various proteasome species are indicated on the far left of the panels (R, RP; C, CP; and b, base). (B) Affinity purification of proteasomes from CP- and base-tagged stains. YYS37 (*PRE1-3xFLAG*) and YYS39 (*RPN1-3xFLAG*), YKN6 (*rpn5-1 PRE1-3xFLAG*) and YKN8 (*rpn5-1 RPN1-3xFLAG*) cells were cultured for 7 h at 37°C and proteasomes were affinity purified from 2 mg of total proteins using anti-FLAG agarose. The purified proteasomes were resolved on a 12.5% SDS-polyacrylamide gel and stained with CBB (left, CP tagged; and right, base tagged). Bands corresponding to the tagged components are indicated with solid arrowheads. The approximate migrating positions of the base and the CP components are indicated by bars on the right side of the panel.

Assembly of the Lid in a Base Mutant ΔN rpn2

In the previous section, we showed that the base was produced independently of the assembly of the lid. Next, we ask the following question: Are the lid and the base assembled independently to each other? To address this issue, we examined the status of lid assembly in a temperature-sensitive base mutant of *RPN2* termed *ΔN rpn2* (equivalent to *rpn2Δ* described by Yokota *et al.* 1996). *ΔN rpn2* is a mutant that carries an N-terminal truncated (Δ1-220aa) version of *RPN2* in a null *rpn2* strain. It stopped growth after 4–6 h at 37°C (data not shown). To see the assembly state in this mutant, total lysates were prepared from *ΔN rpn2* cells grown for 6 h at either 25 or 37°C, and 5 mg of total proteins was resolved on a Superose 6 gel filtration column.

The *ΔN rpn2* mutant was found to have a more severe defect in the structure of proteasomes than the *rpn5-1* mutant, because peptidase assays and Western blotting both showed reduced amount of the 26S holoenzyme even at the permissive temperature (Figure 4, A and B, left). The defects were strongly enhanced when cells were grown at the restrictive temperature. Peptidase activity measurement showed that in *ΔN rpn2* cells incubated at 37°C, the peak corresponding to the 26S proteasome was almost completely lost, and a single high peak of free CPs was detected at fraction no.26 (Figure 4A, right).

Western blotting of chromatographic fractions (Figure 4B, right) revealed that all lid components tested were detected in fraction no.28, which is comparable with the eluting position of a free lid (ca. 500 kDa). These results suggest that in *ΔN rpn2* under the restrictive condition, the lid exists in a free form, unbound to the base. Indeed, this was confirmed by native PAGE (Figure 4C) and affinity purification by using Rpn11p-3xFLAG (lid), by which a complete lid was affinity purified from *ΔN rpn2* cells (Figure 4D, lane 6). The incorporation of all of the nine lid components was verified by band comparison with a wild-type lid and liquid chromatography tandem mass spectrometry (Supplemental Figure 2). It was also shown that a ΔN Rpn2p-less base was formed in *ΔN rpn2* cells at the restrictive temperature (Figure 4D, lane 3). Together with the results of the *rpn5-1* extract, we conclude that the base formation and the lid formation can be independent of each other and are separable processes.

Localization of the Base and the CP in Lid Mutants

In yeast, the 26S proteasome is known to be highly enriched in the nucleus (Wilkinson *et al.*, 1998; Enenkel *et al.*, 1999). Biochemical analysis described above has shown that the lid formation was independent of the base formation. It is not known to date whether the assembly of the base and the lid into an RP is a prerequisite for their nuclear localization. To observe the localization of proteasomes in lid mutants, we generated GFP (Cormack *et al.*, 1996)-fused proteasomes, *PRE6-GFP* (CP), *RPN1-GFP* (base), and *RPN11-GFP* (lid) strains, in which one of the chromosomal *PRE6*, *RPN1*, and *RPN11* genes had been replaced with a C-terminally GFP-tagged gene, and the incorporation of the GFP-fused proteins into the proteasome were verified (Supplemental Figure 3).

Rpn1p-GFP and Pre6p-GFP showed strong nuclear localization in wild-type cells regardless of the incubating temperature (Figure 5A, left; data for 25°C not shown) as reported previously (Enenkel *et al.*, 1999; Wendler *et al.*, 2004). The localization was also examined in two lid mutants, *rpn5-1* and *rpn7-3*, in which the base was not associated with the lid under restrictive conditions. Both base and CP signals were observed in the nucleus regardless of the cultivation conditions (Figure 5A, middle and right), indicating that the *rpn5-1* and *rpn7-3* mutations that perturb the interaction between the lid and the base do not affect the nuclear localization of the base and the CP and that the nuclear localization of the base and the CP is independent of the binding of the lid to the base.

FRAP Experiments

One concern was that the base and CP signals detected at the restrictive temperature might be those of the remaining proteins synthesized and imported under the permissive temperature. To test this possibility, we observed the FRAP, by bleaching the nuclear region with intense laser and observing the recovery of fluorescence after 120 min.

We first carried out an experiment using a wild-type strain producing Rpn1p-GFP instead of Rpn1p. The GFP signals indeed vanished after photobleaching the region of the nucleus (Figure 5B, left and middle). When observed at 120 min after photobleaching, the GFP fluorescence occurred in the nucleus again, proving that nuclear import of the base has occurred (Figure 5B, right). Next, the recovery from photobleaching in *rpn7-3* cells was similarly examined using

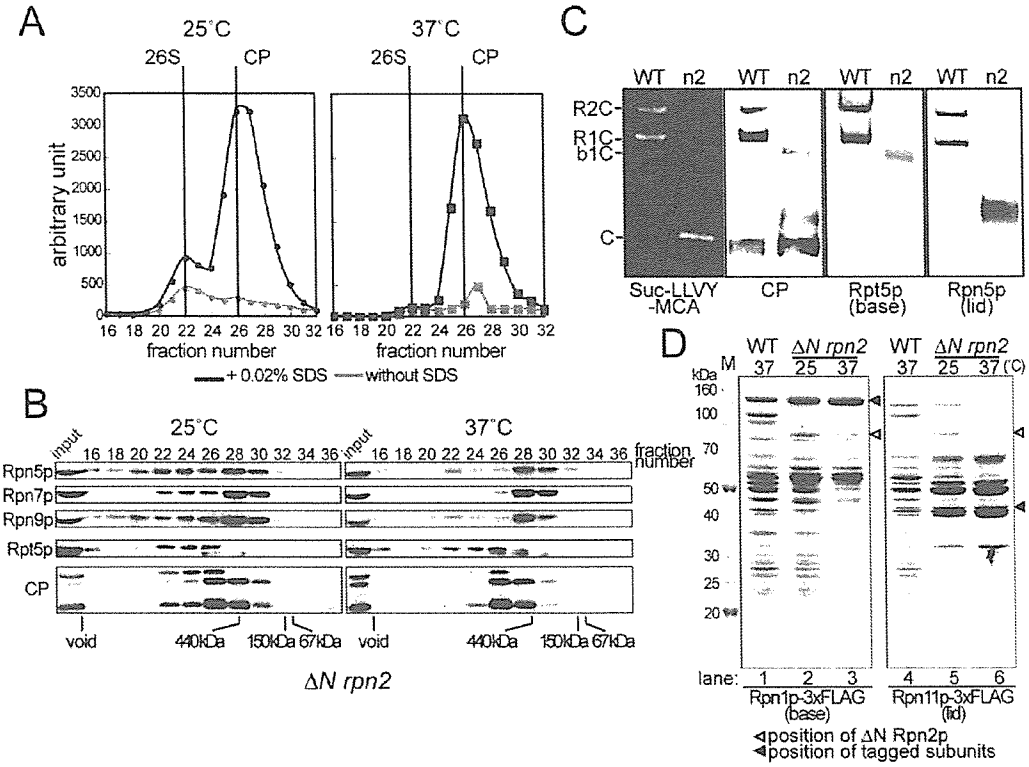

Figure 4. Lid formation does not depend on the binding of the lid to the base. (A) Extract of Δ*N rpn2* (YAT2433) cells cultured for 6 h at 25 or 37°C was resolved on a Superose 6 column, and peptidase activity was measured as described in Figure 2A. Positions of the 26S holoenzyme and the CP are indicated at the top of the graph (black lines, with 0.02% SDS; and gray lines, without SDS). (B) Fractions were subjected to Western blotting as described in Figure 2B. Antibodies used are indicated on the left of the panel (Rpn5p, Rpn7p, and Rpn9p, lid; and Rpt5, base). Positions of the void fraction and marker proteins (ferritin [440 kDa], aldolase [150 kDa], and bovine serum albumin [67 kDa]) are indicated at the bottom of the panels. Note that all lid components examined comigrated. (C) Wild-type (W303-1A) or Δ*N rpn2* (YAT2433) cells were cultured for 6 h at 37°C, and extract was prepared as described above. Extract equivalent to 50 μg of protein was resolved by nondenaturing PAGE. Proteasomes were visualized by overlaying buffer containing 0.1 mM Suc-LLVY-MCA and 0.05% SDS on the gels (far left panel). The same gels were subsequently subjected to Western blotting by using antibodies indicated on the bottom of the panels (Rpt5p, base; and Rpn5p, lid). Bands corresponding to various proteasome species are indicated on the far left of the panels (R, RP; C, CP; and b, base). (D) Affinity purification of proteasomes from base- and lid-tagged strains YYS39 (*RPN1-3xFLAG*), YYS40 (*RPN11-3xFLAG*), YEK234 (Δ*N rpn2 RPN1-3xFLAG*), and YAT3507 (Δ*N rpn2 RPN11-3xFLAG*) cells were cultured for 6 h at 25 or 37°C as indicated, and proteasomes were affinity-purified using anti-FLAG agarose. The purified proteasomes were resolved on a 12.5% SDS-polyacrylamide gel and stained with CBB (left, base tagged; and right, lid tagged). Protein bands were cut out and identified by mass spectrometry (see Supplemental Figure 2). The approximate migrating positions of base and lid components are indicated on the right of the panel (solid arrowhead, tagged component; open arrowhead, ΔN Rpn2p; and M, marker).

rpn7-3 strains expressing *RPN1-YGFP* and *PRE6-YGFP*. Cells were held under the restrictive condition by keeping the glass slides at 37°C by using a stage heater. In *rpn7-3* cells, recovery of both base and CP signals were observed even at the restrictive temperature (Figure 5, C and D). The fluorescence intensity in the nucleus was quantified and the degree of fluorescence recovery in *rpn7-3* cells was found to be comparable with that in the wild-type cells (Figure 5, C and D).

Localization of the Free Lid in ΔN rpn2 Cells

One of the striking features of the Δ*N rpn2* mutant is that its lid exists as a free complex. Because in no known mutant was the lid separated from the base in vivo, it has been difficult to examine whether the lid and the base could be imported into the nucleus independent of each other. We used the Δ*N rpn2* strain to observe the localization of the free lid along with the base by creating its *RPN11-GFP* (lid) or *RPN1-GFP* (base) derivative (Figure 6). Surprisingly, not only the base but also the lid was localized in the nucleus even at 37°C, suggesting that the import of the lid and the base does occur independently. It was verified by gel filtration (Figure 6B) and subsequent immunoprecipitaiton (Figure 6C) that the GFP signals corresponded to the respective complexes. The import of the lid into the nucleus under the restrictive condition was further corroborated by performing FRAP experiments (Figure 6D).

Localization of lid$^{rpn7\text{-}3}$ in rpn7-3 Cells

In the previously characterized *rpn7-3* mutant, it was shown that five of the nine lid components formed a subcomplex termed lid$^{rpn7\text{-}3}$ (Isono *et al.*, 2004). To see whether this partially assembled lid$^{rpn7\text{-}3}$ could be imported into the nucleus, we attempted to analyze the localization of lid$^{rpn7\text{-}3}$ in the *RPN11p-GFP rpn7-3* strain. However, because Rpn11p-GFP was not incorporated into lid$^{rpn7\text{-}3}$ at the restrictive temperature (data not shown), we observed its localization by using the indirect immunofluorescence method. *RPN11-3xFLAG* wild-type and *RPN11-3xFLAG rpn7-3* cells were

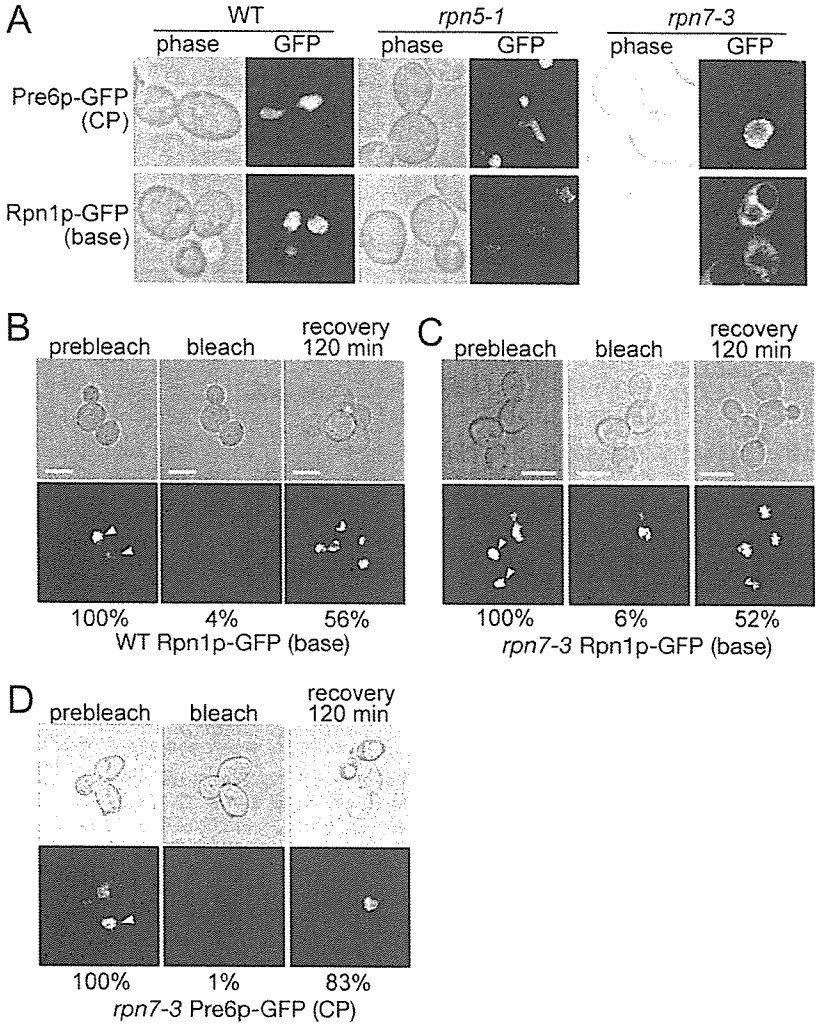

Figure 5. The base and the CP are localized in the nucleus in lid mutants even at the restrictive temperature. (A) Wild-type, *rpn5-1* and *rpn7-3* cells producing Pre6p-GFP (CP) or Rpn1p-GFP (base) instead of the authentic Pre6p and Rpn1p, respectively, were cultured for 7 h at 37°C and photographed under a confocal microscope. Strains used were *PRE6-GFP* (CP), wild type (YEK79), *rpn5-1* (YKN18), *rpn7-3* (YEK211), and *RPN1-GFP* (base) wild type (YEK147), *rpn5-1* (YKN16), *rpn7-3* (YEK213). (B–D) The base and the CP are imported into the nucleus after shift to the restrictive temperature. Rpn1p-GFP (base) producing wild-type (YEK147) and Rpn1p-GFP or Pre6p-GFP (CP) producing *rpn7-3* (YEK213 and YEK211, respectively) cells were cultured for 6 h at 37°C and embedded in agarose as described in *Materials and Methods*. GFP signals in the nucleus (prebleach, left) were photobleached with intense laser (bleach, middle), and FRAP was observed and photographed after 120 min (recovery, right). The stage was kept at 37°C throughout the experiment. Fluorescence intensity ([/mm^2] − background [/mm^2]) was quantified and shown as a relative value to the prebleach intensity at the bottom of each panel. The mean value of two independent experiments is shown. Bar; 5 μm.

cultured for 7 h at 37°C, fixed, and stained. In wild-type cells and *rpn7-3* cells cultured at 25°C, the signal corresponding to the 26S proteasome was clearly nuclear localized, and strong signals at the nuclear periphery was observed (Figure 7A, second and third panels from the top; data for 25°C wild-type samples not shown). On the contrary, in *rpn7-3* cells cultured at 37°C, the nuclear localization was not seen, and signals of DAPI-stained DNA did not merge with the FLAG signals any more (Figure 7A, lowermost panel), showing that the lid$^{rpn7\text{-}3}$ was not localized in the nucleus.

To confirm this observation, immunostaining was also performed using an antibody against Rpn5p, one of the components of lid$^{rpn7\text{-}3}$. Again, the nuclear localization seen in wild type cells could not be observed in the *rpn7-3* cells, in which signals of Rpn5p were detected dispersed in the cytosol (Figure 7B). This result suggests that the lid is built up in the cytosol and then imported into the nucleus to be assembled into the 26S complex, although we cannot exclude the possibility that the lid$^{rpn7\text{-}3}$ is reexported to the cytosol after carried into the nucleus. The structure of the nucleus itself was not damaged in *rpn7-3* cells under the restrictive condition, which was verified by the normal localization of mRFP (Campbell *et al.*, 2002) fused Nup53p, a component of the nuclear pore complex, in wild-type and also in *rpn7-3* cells at 37°C (Figure 7C).

From the above-mentioned results, we anticipated that the components not included in the lid$^{rpn7\text{-}3}$, namely, Rpn3p, Rpn7p, Rpn12p, and Rpn15p, might be responsible for the import of the lid. To test this possibility, we expressed one of the GFP-fused constructs of *RPN3*, *RPN7*, *RPN12*, or *RPN15* under their native promoters in *rpn5-1* cells. The cells were cultured for 7 h at 37°C and GFP signals were observed under a confocal microscope (Figure 7D). Rpn3p, Rpn7p, and Rpn12p showed nuclear localization, whereas Rpn15p did not, showing that Rpn3p, Rpn7p, and Rpn12p can be localized in the nucleus as monomers under these conditions.

The Nuclear Import of the Lid Does Not Depend on Srp1p

Srp1p, karyopherin α, was reported to be involved in the import of proteasomes into the nucleus (Tabb *et al.*, 2000; Lehmann *et al.*, 2002; Wendler *et al.*, 2004). In accordance with previous reports, in a temperature-sensitive mutant of *SRP1* termed *srp1-49*, Rpn11p-GFP (lid) and Rpn1p-GFP (base) were delocalized (Supplemental Figure 4). However, because no method has been available to form the lid and

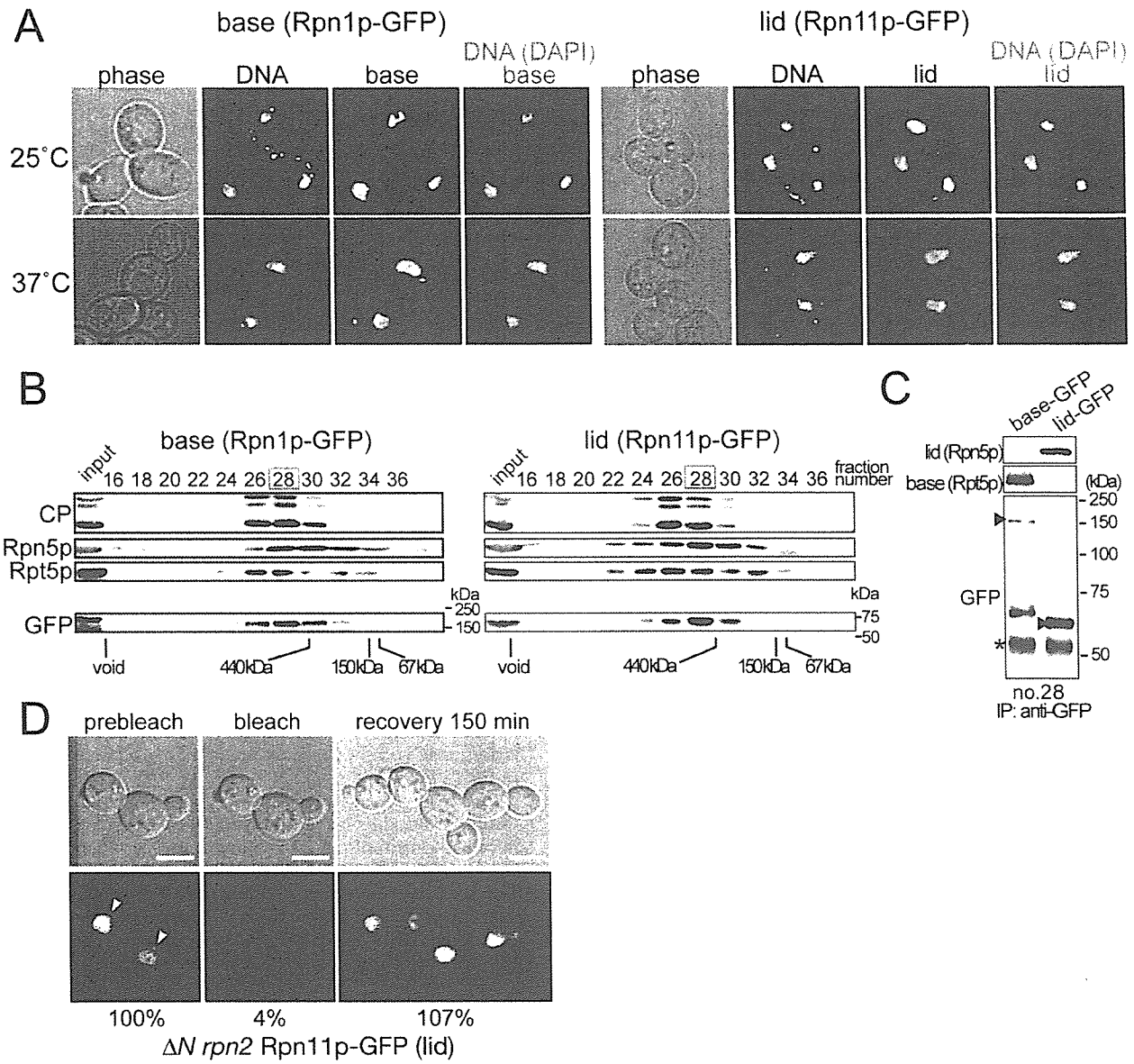

Figure 6. The nuclear import of the base and the lid are independent of each other. (A) Δ*N rpn2* cells producing Rpn1p-GFP (base, YEK235) or Rpn11p-GFP (lid, YEK236) instead of the authentic Rpn1p or Rpn11p, respectively, were cultured for 6 h at either 25 or 37°C and photographed under a confocal microscope. DNA was stained with Hoechst 33342. (B) Total proteins were extracted from the cells cultured at 37°C as described in A and subjected to gel filtration by using a Superose 6 column. Fractions were subsequently subjected to Western blotting by using the antibodies indicated on the left of the panels. (Rpn5p; lid, Rpt5p; base) Positions of the void fraction and marker proteins (ferritin [440 kDa], aldolase [150 kDa], and bovine serum albumin [67 kDa]) are indicated at the bottom of the panels. For the GFP blot, positions of molecular mass markers are shown on the right of each of the panels. (C) Immunoprecipitation was performed against fraction 28 in B by using anti-GFP antibody and analyzed by Western blotting by using anti-Rpn5p (lid), anti-Rpt5p (base), and anti-GFP antibodies. Asterisks indicate nonspecific bands. Arrowheads indicate the GFP-fused components. (D) *RPN11-GFP*–expressing Δ*N rpn2* (YEK256) cells were cultured for 6 h at 37°C, and FRAP experiments were performed as in Figure 5, except that the recovery was observed after 150 min. Fluorescence intensity ([/mm^2] − background [/mm^2]) was quantified and shown as relative values to the prebleach intensity at the bottom of each panel. The mean value of two independent experiments is shown. Arrowheads indicate the cell that was photobleached. Bar; 5 μm.

the base separately in vivo, it had been impossible to examine whether their nuclear import would be dependent on Srp1p.

To address this issue, we took advantage of the Δ*N rpn2* mutant, in which the lid exists as a free complex at the restrictive temperature. Either *RPN7-GFP* or *RPN1-GFP* was introduced into the Δ*N rpn2 srp1-49* double mutant to replace each of the authentic genes. Cells were cultured for 8 h at 37°C and observed under a confocal microscope. Although the base lost its strong nuclear localization seen at 25°C, and a part of the signals was dispersed in the cytosol, the lid signals remained strongly in the nucleus at 37°C (Figure 8A), which was corroborated by the quantification of the fluorescence signals (Figure 8B). These results suggest

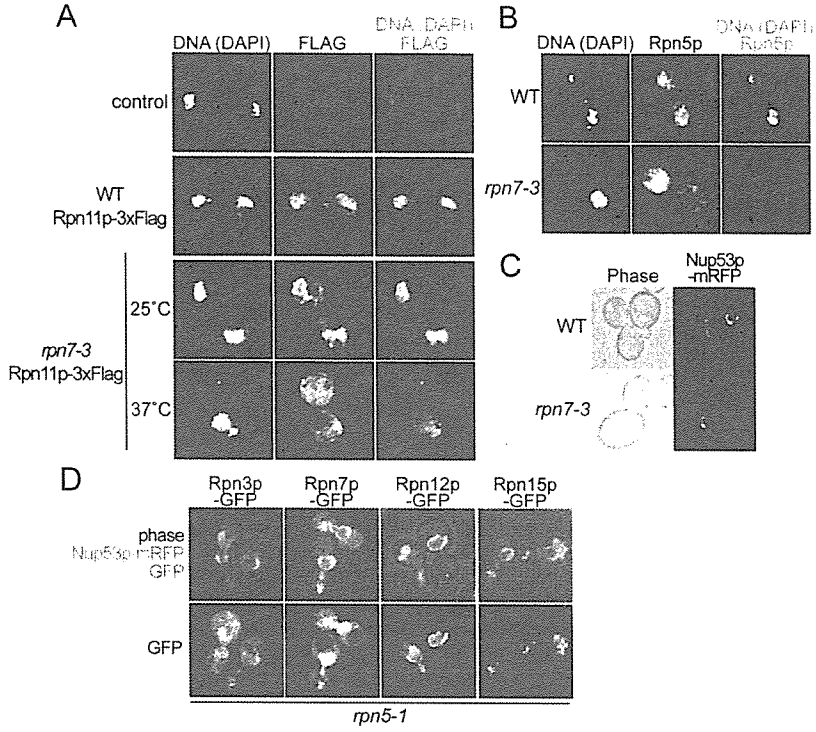

Figure 7. Localization of the partially assembled lid$^{rpn7\text{-}3}$. (A) *RPN11-3xFLAG* (YYS40) and *rpn7-3 RPN11-3xFLAG* (YEK29) cells, along with untagged wild-type (W303-1A) cells, were cultured for 6 h at 25 or 37°C as indicated, and localization of lid$^{rpn7\text{-}3}$ was detected by the indirect immunofluorescence method by using anti-FLAG M2 antibody. Photographs were taken under a confocal microscope. DNA was stained with DAPI. (B) Wild-type (W303-1B) and *rpn7-3* (YEK6) cells were incubated for 6 h at 37°C, and localization of Rpn5p was detected as described in A by the indirect immunofluorescence method except that an anti-Rpn5p antibody was used. DNA was stained with DAPI. (C) The nuclear envelope is normal in *rpn7-3* cells under the restrictive condition. Nup53p-mRFP (pEK285) was produced in wild-type (W303-1A) and *rpn7-3* (YEK6) cells cultured at the same condition as described in B and photographed under a confocal microscope. (D) Localization of Rpn3p-GFP (pEK297), Rpn7p-GFP (pEK298), Rpn12p-GFP (pEK299), or Rpn15p-GFP (pEK300) in *rpn5-1* (YEK100) cells. Cells were cultured for 8 h at 37°C, and GFP signals were photographed under a confocal microscope. Nup53p-mRFP was used as a marker for the nuclear envelope.

that the nuclear import of the base is dependent on Srp1p, whereas that of the lid does not.

DISCUSSION

The *RPN5* gene, originally named *non-ATPase subunit 5* (*NAS5*), is an essential gene in *S. cerevisiae*, in contrast to *Schizosaccharomyces pombe*, and is a homologue of human p55 (Finley *et al.*, 1998). In this study, we have shown that in *rpn5-1* cells, not even a partially assembled subcomplex of the lid was detected at the restrictive temperature (Figure 2, B–D). This result, together with our previous reports, indicates that the mutation in Rpn5p inhibits the complex formation of the lid, and thus Rpn5p is a key component in the core formation of the lid. A very recently published report has shown the interaction between subunits of the RP by tandem MS analysis (Sharon *et al.*, 2006). Using this novel approach, it was demonstrated that Rpn5p, Rpn8p, Rpn9p, and Rpn11p is forming a stable soluble subcomplex and a subunit interaction map was proposed, which is in good accordance with our results that Rpn5p is a core component in lid formation.

Interestingly, the addition of a 3xFLAG tag at the C terminus to another lid component Rpn11p rescued the temperature-sensitivity of *rpn5-1* and at the same time its defect in assembling the 26S proteasome (Supplemental Figure 6). Probably, the C terminus of Rpn11p is located near to the C terminus of Rpn5p so that its extension suppresses the structural alternation of the proteasome caused by the incorporation of the truncated Rpn5-1p. Because the structural recovery of the 26S proteasome led to a complete growth recovery at the restrictive temperature, the *rpn5-1* mutation was probably causing purely structural defects.

The fact that the base-CP interaction in mutant cells is unstable indicates the possibility that the lid functions to strengthen the base-CP binding by allosterically affecting the base-CP interface. This result is in contrast to a previous report in which a base-CP complex was purified from a mutant of *RPN11* termed *mpr1–1* in the absence of the lid

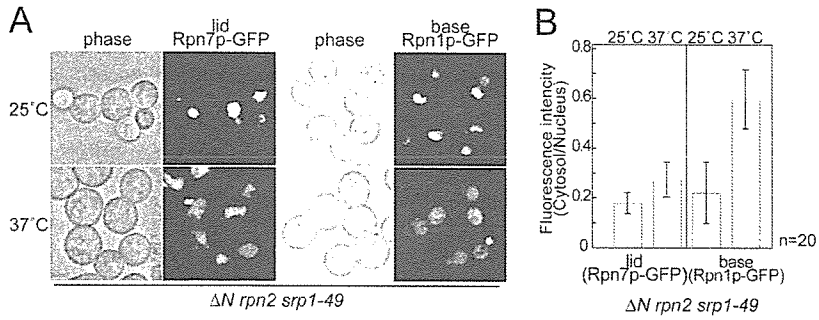

Figure 8. Nuclear localization of the base, but not the lid, is affected by *srp1-49*. (A) Δ*N rpn2 srp1-49* cells expressing Rpn7p-GFP or Rpn1p-GFP (YEK247 and YEK258, respectively) were cultured for 8 h at either 25 or 37°C, and localization of the GFP-fused components was observed under a confocal microscope. (B) Signals of A were quantified (fluorescence intensity per area) using the IPLab software, and ratio of the nuclear and cytosolic signals is shown. Error bars represent SD (n = 20).

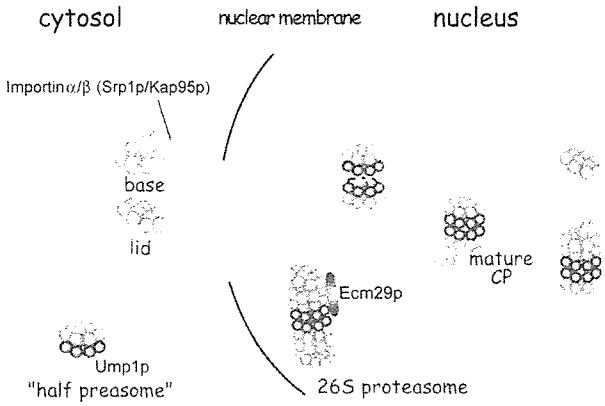

Figure 9. Model for the assembling process of the 26S proteasome in budding yeast. The base and the lid are made in the cytosol and are imported into the nucleus independently. On the dimerization of half-proteasomes into a mature CP, the base binds the CP. The immediate binding of the lid to the base–CP complex stabilizes the whole complex. Additional interacting proteins are bound to the 26S proteasome.

(Verma *et al.*, 2002). We have no explanation for this discrepancy at present.

In fission yeast, it was proposed that SpRpn5, together with the human breast cancer related gene Int6/Yin6, serves for the nuclear localization of the lid (Yen *et al.*, 2003b), although our results showed that the lid$^{rpn7\text{-}3}$ containing Rpn5p was not localized in the nucleus (Figure 7, A and B). One explanation of these seemingly controversial results may be that there is no Int6/Yin6 homologue in budding yeast and hence the Int6/Yin6 associated function of Rpn5p is not conserved in the two yeast species.

The CP and an interacting ATPase exist already in prokaryotic organisms. Given that the lid shares its origin with COP9/signalosme and eIF3, both of which are functioning as a single complex, it is reasonable that the formation and the nuclear localization of the base and the lid are independent to each other. However, although the base is imported into the nucleus via the Srp1p-dependent importin α/β pathway, the lid seems to be carried into the nucleus via another system that is independent of Srp1p (Figure 8, A and B). As for the base, two of the base components, Rpn2p and Rpt2p, were shown to possess functional nuclear localization signal (NLS) sequences, and because the simultaneous deletion of these sequences is lethal, it was suggested that the nuclear import of the base probably depends on its own NLS(s) (Wendler *et al.*, 2004). No component of the lid was yet proved to be responsible for the nuclear import of the lid. Our results suggest that Rpn3p, Rpn7p, and Rpn12, each of which is localized into nucleus by itself, may serve for the nuclear import of the lid (Figure 7D).

We have shown in this study that the lid, a substructure of the 26S proteasome, can be formed and imported into the nucleus independently of the other subcomplexes of the 26S proteasome. Together with the result that a base–CP complex is formed in the analyzed lid mutants, we propose the following scenario of the assembling pathway of the 26S proteasome (Figure 9). The half-proteasome as well as base and the lid are formed independently in the cytosol, and they are imported into the nucleus. Then, the base binds the mature CP, and finally the lid binds the base–CP complex to form a mature 26S proteasome. In the course of the formation of the lid, Rpn5p, together with its interacting components forms the core of the lid, into which Rpn6p then the rest of the components are sequentially incorporated to become a complete lid. It should be noted that the scenario of the assembly pathway described above had been drawn using mutants, and there might be a different pathway in wild-type cells. In wild-type cells, the assembly processes are probably too rapid to be detected biochemically, because the apparent intermediates of the 26S proteasome such as the base–CP complex, lid$^{rpn6\text{-}1}$ and lid$^{rpn7\text{-}3}$ existed in lid mutants under the restrictive condition (Isono *et al.*, 2004, 2005) cannot be detected.

This consideration casts another question as to whether there are any factors that facilitate or regulate the interaction between the base, lid and CP. It should be noted that a recent report with mammalian cells has shown that a protein interacting with the ATPase subunits of the base, named PAAF1, inhibits the binding of the RP and the CP (Park *et al.*, 2005). Whether external factors are involved in the formation of the lid and the base is also a question that remains to be answered.

ACKNOWLEDGMENTS

We thank Dr. Daniel Finley (Harvard University, Boston, MA) for the anti-Rpn8p antibody, Dr. Jussi Jantti (University of Helsinki, Helsinki, Finland) for the anti-Sem1p (Rpn15p) antibody, and Dr. Roger Tsien (University of California, San Diego, San Diego, CA) for the mRFP1 plasmid. We are grateful to Dr. Cordula Enenkel (Humboldt University, Berlin, Germany) for valuable suggestions and advice, Drs. Satoshi Yoshida (Harvard University, Boston, MA) and Takashi Itoh (RIKEN, Saitama, Japan) for technical advice, and the members of the Laboratory of Genetics for discussions and comments. Thanks are also due to Drs. Yoshibumi Komeda and Ichiro Terashima (University of Tokyo, Tokyo, Japan) for generously letting us use the laboratory space and to Naoko Saito for earlier contribution to this work. This work was supported by a grant-in-aid for scientific research from the Ministry of Education, Culture, Sports, Science, and Technology (to A.T.) and by a grant-in-aid from the Japan Society for Promotion of Young Scientists (to E.I.).

REFERENCES

Bachmair, A., Finley, D., and Varshavsky, A. (1986). In vivo half-life of a protein is a function of its amino-terminal residue. Science *234*, 179–186.

Burk, D., Dawson, D., and Stearns, T. (2000). Methods in Yeast Genetics. Cold Spring Harbor, NY: Cold Spring Harbor Laboratory Press.

Cadwell, R. C., and Joyce, G. F. (1992). Randomization of genes by PCR mutagenesis. PCR Methods Appl. 2, 28–33.

Campbell, R. E., Tour, O., Palmer, A. E., Steinbach, P. A., Baird, G. S., Zacharias, D. A., and Tsien, R. Y. (2002). A monomeric red fluorescent protein. Proc. Natl. Acad. Sci. USA *99*, 7877–7882.

Chen, P., and Hochstrasser, M. (1996). Autocatalytic subunit processing couples active site formation in the 20S proteasome to completion of assembly. Cell *86*, 961–972.

Cope, G. A., Suh, G. S., Aravind, L., Schwarz, S. E., Zipursky, S. L., Koonin, E. V., and Deshaies, R. J. (2002). Role of predicted metalloprotease motif of Jab1/Csn5 in cleavage of Nedd8 from Cul1. Science *298*, 608–611.

Cormack, B. P., Valdivia, R. H., and Falkow, S. (1996). FACS-optimized mutants of the green fluorescent protein (GFP). Gene *173*, 33–38.

Elsasser, S., Chandler-Militello, D., Muller, B., Hanna, J., and Finley, D. (2004). Rad23 and Rpn10 serve as alternative ubiquitin receptors for the proteasome. J. Biol. Chem. *279*, 26817–26822.

Enenkel, C., Lehmann, A., and Kloetzel, P. M. (1999). GFP-labelling of 26S proteasomes in living yeast: insight into proteasomal functions at the nuclear envelope/rough ER. Mol. Biol. Rep. *26*, 131–135.

Fehlker, M., Wendler, P., Lehmann, A., and Enenkel, C. (2003). Blm3 is part of nascent proteasomes and is involved in a late stage of nuclear proteasome assembly. EMBO Rep. *4*, 959–963.

Finley, D., *et al.* (1998). Unified nomenclature for subunits of the *Saccharomyces cerevisiae* proteasome regulatory particle. Trends Biochem. Sci. *23*, 244–245.

Fu, H., Reis, N., Lee, Y., Glickman, M. H., and Vierstra, R. D. (2001). Subunit interaction maps for the regulatory particle of the 26S proteasome and the COP9 signalosome. EMBO J. *20*, 7096–7107.

Funakoshi, M., Li, X., Velichutina, I., Hochstrasser, M., and Kobayashi, H. (2004). Sem1, the yeast ortholog of a human BRCA2-binding protein, is a component of the proteasome regulatory particle that enhances proteasome stability. J. Cell Sci. *117*, 6447–6454.

Glickman, M. H., Rubin, D. M., Coux, O., Wefes, I., Pfeifer, G., Cjeka, Z., Baumeister, W., Fried, V. A., and Finley, D. (1998a). A subcomplex of the proteasome regulatory particle required for ubiquitin-conjugate degradation and related to the COP9-signalosome and eIF3. Cell *94*, 615–623.

Glickman, M. H., Rubin, D. M., Fried, V. A., and Finley, D. (1998b). The regulatory particle of the *Saccharomyces cerevisiae* proteasome. Mol. Cell Biol. *18*, 3149–3162.

Guterman, A., and Glickman, M. H. (2004). Complementary roles for Rpn11 and Ubp6 in deubiquitination and proteolysis by the proteasome. J. Biol. Chem. *279*, 1729–1738.

Hershko, A., and Ciechanover, A. (1998). The ubiquitin system. Annu. Rev. Biochem. *67*, 425–479.

Hirano, Y., Hendil, K. B., Yashiroda, H., Iemura, S., Nagane, R., Hioki, Y., Natsume, T., Tanaka, K., and Murata, S. (2005). A heterodimeric complex that promotes the assembly of mammalian 20S proteasomes. Nature *437*, 1381–1385.

Hoepfner, D., Brachat, A., and Philippsen, P. (2000). Time-lapse video microscopy analysis reveals astral microtubule detachment in the yeast spindle pole mutant cnm67. Mol. Biol. Cell *11*, 1197–1211.

Hofmann, K., and Bucher, P. (1998). The PCI domain: a common theme in three multiprotein complexes. Trends Biochem. Sci. *23*, 204–205.

Isono, E., Saeki, Y., Yokosawa, H., and Toh-e, A. (2004). Rpn7 Is required for the structural integrity of the 26 S proteasome of *Saccharomyces cerevisiae*. J. Biol. Chem. *279*, 27168–27176.

Isono, E., Saito, N., Kamata, N., Saeki, Y., and Toh, E. A. (2005). Functional analysis of Rpn6p, a lid component of the 26 S proteasome, using temperature-sensitive rpn6 mutants of the yeast *Saccharomyces cerevisiae*. J. Biol. Chem. *280*, 6537–6547.

Leggett, D. S., Hanna, J., Borodovsky, A., Crosas, B., Schmidt, M., Baker, R. T., Walz, T., Ploegh, H., and Finley, D. (2002). Multiple associated proteins regulate proteasome structure and function. Mol. Cell *10*, 495–507.

Lehmann, A., Janek, K., Braun, B., Kloetzel, P. M., and Enenkel, C. (2002). 20 S proteasomes are imported as precursor complexes into the nucleus of yeast. J. Mol. Biol. *317*, 401–413.

Maytal-Kivity, V., Reis, N., Hofmann, K., and Glickman, M. H. (2002). MPN+, a putative catalytic motif found in a subset of MPN domain proteins from eukaryotes and prokaryotes, is critical for Rpn11 function. BMC Biochem. *3*, 28.

Park, Y., Hwang, Y. P., Lee, J. S., Seo, S. H., Yoon, S. K., and Yoon, J. B. (2005). Proteasomal ATPase-associated factor 1 negatively regulates proteasome activity by interacting with proteasomal ATPases. Mol. Cell Biol. *25*, 3842–3853.

Ramos, P. C., Hockendorff, J., Johnson, E. S., Varshavsky, A., and Dohmen, R. J. (1998). Ump1p is required for proper maturation of the 20S proteasome and becomes its substrate upon completion of the assembly. Cell *92*, 489–499.

Saeki, Y., Isono, E., and Toh-e, A. (2005). Preparation of ubiquitinated substrates by the PY motif-insertion method for monitoring 26S proteasome activity. Methods Enzymol. *399*, 215–227.

Saeki, Y., Saitoh, A., Toh-e, A., and Yokosawa, H. (2002). Ubiquitin-like proteins and Rpn10 play cooperative roles in ubiquitin-dependent proteolysis. Biochem. Biophys. Res. Commun. *293*, 986–992.

Sasaki, T., Toh-e, A., and Kikuchi, Y. (2000). Yeast Krr1p physically and functionally interacts with a novel essential Kri1p, and both proteins are required for 40S ribosome biogenesis in the nucleolus. Mol. Cell. Biol. *20*, 7971–7979.

Schmidt, M., Haas, W., Crosas, B., Santamaria, P. G., Gygi, S. P., Walz, T., and Finley, D. (2005). The HEAT repeat protein Blm10 regulates the yeast proteasome by capping the core particle. Nat. Struct. Mol. Biol. *12*, 294–303.

Schwartz, A. L., and Ciechanover, A. (1999). The ubiquitin-proteasome pathway and pathogenesis of human diseases. Annu. Rev. Med. *50*, 57–74.

Sharon, M., Taverner, T., Ambroggio, X. I., Deshaies, R. J., and Robinson, C. V. (2006). Structural organization of the 19S proteasome lid: insights from MS of intact complexes. PLoS Biol. *4*.

Sherman, F., Fink, G. R., and Hicks, J. B. (1986). Methods in Yeast Genetics, Cold Spring Harbor, NY: Cold Spring Harbor Laboratory Press, 12–18.

Sikorski, R. S., and Hieter, P. (1989). A system of shuttle vectors and yeast host strains designed for efficient manipulation of DNA in *Saccharomyces cerevisiae*. Genetics *122*, 19–27.

Sone, T., Saeki, Y., Toh-e, A., and Yokosawa, H. (2004). Sem1p is a novel subunit of the 26 S proteasome from *Saccharomyces cerevisiae*. J. Biol. Chem. *279*, 28807–28816.

Tabb, M. M., Tongaonkar, P., Vu, L., and Nomura, M. (2000). Evidence for separable functions of Srp1p, the yeast homolog of importin alpha (Karyopherin alpha): role for Srp1p and Sts1p in protein degradation. Mol. Cell Biol. *20*, 6062–6073.

Takeda, K., and Yanagida, M. (2005). Regulation of nuclear proteasome by Rhp6/Ubc2 through ubiquitination and destruction of the sensor and anchor Cut8. Cell *122*, 393–405.

Tatebe, H., and Yanagida, M. (2000). Cut8, essential for anaphase, controls localization of 26S proteasome, facilitating destruction of cyclin and Cut2. Curr. Biol. *10*, 1329–1338.

Toh-e, A., and Oguchi, T. (2000). An improved integration replacement/disruption method for mutagenesis of yeast essential genes. Genes Genet. Syst. *75*, 33–39.

van Nocker, S., Sadis, S., Rubin, D. M., Glickman, M., Fu, H., Coux, O., Wefes, I., Finley, D., and Vierstra, R. D. (1996). The multiubiquitin-chain-binding protein Mcb1 is a component of the 26S proteasome in *Saccharomyces cerevisiae* and plays a nonessential, substrate-specific role in protein turnover. Mol. Cell Biol. *16*, 6020–6028.

Verma, R., Aravind, L., Oania, R., McDonald, W. H., Yates, J. R., 3rd, Koonin, E. V., and Deshaies, R. J. (2002). Role of Rpn11 metalloprotease in deubiquitination and degradation by the 26S proteasome. Science *298*, 611–615.

Wendler, P., Lehmann, A., Janek, K., Baumgart, S., and Enenkel, C. (2004). The bipartite nuclear localization sequence of Rpn2 is required for nuclear import of proteasomal base complexes via karyopherin $\alpha\beta$ and proteasome functions. J. Biol. Chem. *279*, 37751–37762.

Wilkinson, C. R., Wallace, M., Morphew, M., Perry, P., Allshire, R., Javerzat, J. P., McIntosh, J. R., and Gordon, C. (1998). Localization of the 26S proteasome during mitosis and meiosis in fission yeast. EMBO J. *17*, 6465–6476.

Yao, T., and Cohen, R. E. (2002). A cryptic protease couples deubiquitination and degradation by the proteasome. Nature *419*, 403–407.

Yen, H. C., Espiritu, C., and Chang, E. C. (2003a). Rpn5 is a conserved proteasome subunit and required for proper proteasome localization and assembly. J. Biol. Chem. *278*, 30669–30676.

Yen, H. C., Gordon, C., and Chang, E. C. (2003b). *Schizosaccharomyces pombe* Int6 and Ras homologs regulate cell division and mitotic fidelity via the proteasome. Cell *112*, 207–217.

Yokota, K., *et al.* (1996). CDNA cloning of p112, the largest regulatory subunit of the human 26s proteasome, and functional analysis of its yeast homologue, sen3p. Mol. Biol. Cell *7*, 853–870.

nature
structural &
molecular biology

Direct interactions between NEDD8 and ubiquitin E2 conjugating enzymes upregulate cullin-based E3 ligase activity

Eri Sakata[1], Yoshiki Yamaguchi[1], Yasuhiro Miyauchi[2], Kazuhiro Iwai[2], Tomoki Chiba[3], Yasushi Saeki[4], Noriyuki Matsuda[4], Keiji Tanaka[4] & Koichi Kato[1,5]

Although cullin-1 neddylation is crucial for the activation of SCF ubiquitin E3 ligases, the underlying mechanisms for NEDD8-mediated activation of SCF remain unclear. Here we demonstrate by NMR and mutational studies that NEDD8 binds the ubiquitin E2 (UBC4), but not NEDD8 E2 (UBC12). Our data imply that NEDD8 forms an active platform on the SCF complex for selective recruitment of ubiquitin-charged E2s in collaboration with RBX1, and thereby upregulates the E3 activity.

The SKP1/cullin-1/F-box protein (SCF) complex is a multisubunit ubiquitin E3 ligase that promotes ubiquitination of many important regulatory proteins of diverse cellular pathways (see recent review[1]). Cullin-1, together with the RING-finger protein RBX1 (also called ROC1), forms the catalytic core of the SCF complex. The E3 activity of the SCF complex is modulated by the covalent attachment of the ubiquitin-like molecule NEDD8 to cullin-1 (refs. 2–5). This 'neddylation' pathway is considered essential for cell viability in various organisms, though not in budding yeast[3]. In the neddylation process, the APP-BP1–UBA3 heterodimer (NEDD8 E1) and UBC12 (NEDD8 E2) catalyze the formation of an isopeptide bond between the C-terminal glycine residue of NEDD8 and a lysine residue in the cullin homology domain, whereas the COP9 signalosome catalyzes deneddylation[6]. *In vitro* experiments indicate that cullin-1 neddylation upregulates the E3 activity of the SCF complex and thereby enhances protein ubiquitination[2–5]. Furthermore, it has been shown that this modification is important for the recruitment of E2 to the SCF complex[7,8]. However, the underlying mechanisms of the activation of the SCF complex, through the enhancement of E2 recruitment upon neddylation of cullin-1, remain to be understood. We examined the possible interaction of human NEDD8 with human UBC4, which is an E2 enzyme that catalyzes the formation of polyubiquitin chains upon neddylation of cullin-1 (ref. 7).

^{1}H-^{15}N HSQC spectral analyses of isotopically labeled NEDD8 in the presence and absence of unlabeled UBC4 showed chemical shift perturbations of amide resonances for Thr7, Leu8, Ile44, Ser46, Gly47, Lys48, Gln49, Met50, Val70, Leu71 and Leu73, indicating that NEDD8 interacts with UBC4 through its Ile44 hydrophobic patch (**Fig. 1a**, **Supplementary Fig. 1** and **Supplementary Methods** online). In similar titration experiments using UBC12 instead of UBC4, no

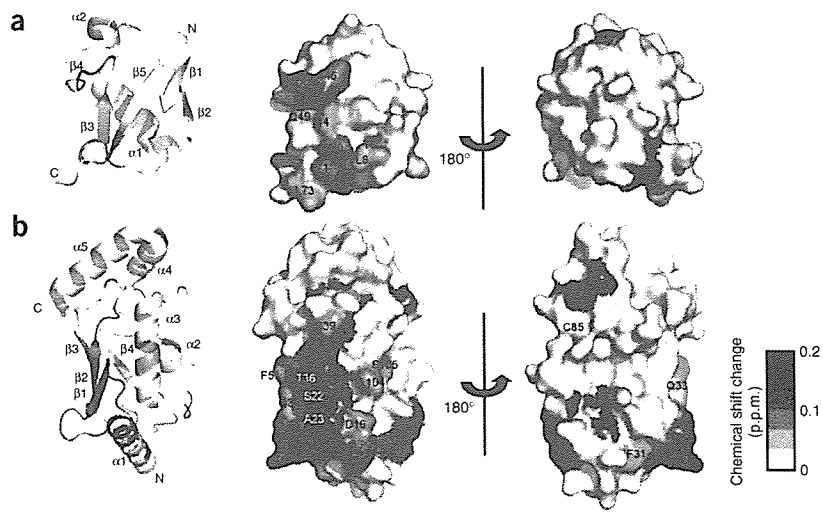

Figure 1 Identification of the binding sites on NEDD8 and UBC4. (**a**,**b**) Mapping of the perturbed residues of NEDD8 (**a**) and UBC4 (**b**) upon binding to each other. Residues are highlighted in red on the crystal structures of NEDD8 (PDB 1NDD) and UBC4 (PDB 2ESK). Red gradient indicates the strength of the perturbation. Blue, residues involved in the interaction with the RING-finger domain in the crystal structure of c-Cbl (PDB 1FBV)[10]; gray, prolines; yellow, catalytic cysteine (C85). This figure was prepared with PyMOL (http://pymol.sourceforge.net).

[1]Department of Structural Biology and Biomolecular Engineering, Graduate School of Pharmaceutical Sciences, Nagoya City University, 3-1 Tanabe-dori, Mizuho-ku, Nagoya 467-8603, Japan. [2]Department of Molecular Cell Biology, Graduate School of Medicine, Osaka City University, 1-4-3 Asahi-machi, Abeno-ku, Osaka 545-8585, Japan. [3]Department of Molecular Biology, Graduate School of Life and Environmental Sciences, University of Tsukuba, 1-1-1 Tennodai, Tsukuba, Ibaraki 305-8577, Japan. [4]Laboratory of Frontier Science, The Tokyo Metropolitan Institute of Medical Science, 3-18-22 Honkomagome, Bunkyo-ku, Tokyo 113-8613, Japan. [5]Institute for Molecular Science, National Institutes of Natural Sciences, 5-1 Higashiyama, Myodaiji, Okazaki, Aichi 444-8787, Japan. Correspondence should be addressed to K.K. (kkato@phar.nagoya-cu.ac.jp).

Received 20 August 2006; accepted 12 December 2006; published online 7 January 2007; doi:10.1038/nsmb1191

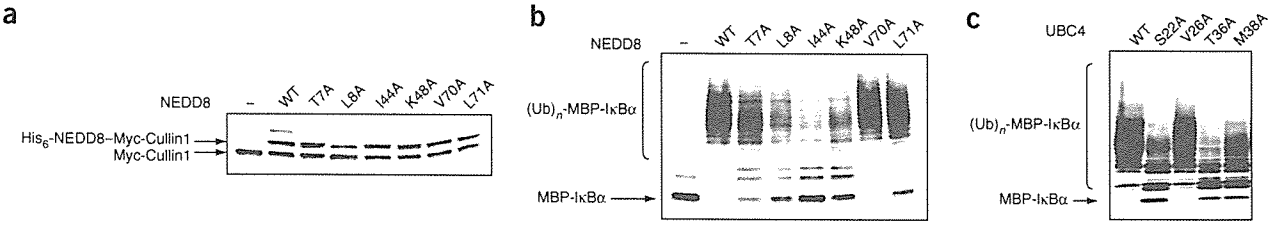

Figure 2 Mutations affecting the NEDD8 and UBC4 interaction compromise upregulation of the E3 activity of $SCF^{\beta\text{-}TrCP1}$ in the ubiquitination of IκBα. (**a**) Effects of NEDD8 mutations on *in vitro* neddylation of cullin-1. (**b**,**c**) Effects of mutations of NEDD8 (**b**) and UBC4 (**c**) on ubiquitination of phosphorylated IκBα. Ubiquitination (symbolized by $(UB)_n$, where *n* represents number of ubiquitins) of a maltose-binding protein (MBP)-IκBα fusion construct by $SCF^{\beta\text{-}TrCP1}$ was examined in the presence or absence of NEDD8 or UBC4 mutants. MBP-IκBα prephosphorylated by IKKβ was used as a substrate.

specific interaction was detected between NEDD8 and UBC12 (**Supplementary Fig. 1**). Next, we identified the NEDD8-binding surface on UBC4. Binding of NEDD8 induced chemical shift perturbations of NMR signals for α1 helix (Leu10, Asp12, Ala14 and Arg15), α1-β1 loop (Asp16, Ala19 and Gln20), β1 strand (Cys20–Ala23), β1-β2 loop (Val26–Phe31) and β2 strand (Trp33–Thr36, Met38 and Gly39) of UBC4 (**Fig. 1b** and **Supplementary Fig. 2** online).

To address the functional relevance of the interaction observed between NEDD8 and UBC4, we mutated the amino acid residues located in the UBC4-binding site of NEDD8 (T7A, L8A, I44A, K48A, V70A and L71A). Whereas these NEDD8 mutants as well as the wild-type NEDD8 were conjugated to cullin-1 to similar extents by *in vitro* neddylation reactions (**Fig. 2a**), an *in vitro* ubiquitination assay revealed differential modulation of their abilities to upregulate the E3 activity of $SCF^{\beta\text{-}TrCP1}$ (substrate-recognition subunit indicated by superscript text) in ubiquitination of IκBα. Notably, the I44A mutant completely lacked the ability to activate this ligase (**Fig. 2b**). An NMR titration experiment confirmed that amino acid substitution of Ile44 with alanine in NEDD8 resulted in loss of its affinity for UBC4 (**Supplementary Fig. 2**). Reciprocally, certain UBC4 mutants with a single amino acid substitution in the NEDD8-binding site (typified by S22A) could not interact with NEDD8 (**Supplementary Fig. 1**) or promote the E3 activity of the neddylated $SCF^{\beta\text{-}TrCP1}$ for ubiquitination of IκBα (**Fig. 2c**), even though these UBC4 mutants had E2 activities comparable to the wild-type UBC4 in *in vitro* ubiquitination reactions with the RMA1 (RING-type) and RSP5 (HECT-type) E3 ligases (**Supplementary Fig. 3** online).

A previous X-ray crystallographic study of SCF^{Skp2} has shown that the neddylation site is in close spatial proximity to the RING-finger domain of RBX1 (ref. 9). The present NMR data suggest that the NEDD8-binding site is distinct from but adjoins the putative RING-binding site on UBC4 (**Fig. 1b**)[10]. On the basis of these data, we propose that NEDD8 provides a hydrophobic surface area for its interaction with the E2 surface area remote from Cys85, the catalytic cysteine, and thereby enhances recruitment of the ubiquitin-charged E2 in collaboration with RBX1. Furthermore, we found that the I44A mutant of NEDD8 did not facilitate the reaction whereby VBC-CUL2 ligase (together with UBCH5c) ubiquitinates its native substrate, indicating that NEDD8-ubiquitin E2 interactions contribute to upregulation of not only cullin-1–based but also cullin-2–based E3 ligase activities (**Supplementary Fig. 4** online).

RBX1 could induce neddylation as well as ubiquitination by allowing alternative binding of different E2s[11]. Our data demonstrate that NEDD8 interacts with the ubiquitin E2, UBC4, but not with the NEDD8 E2, UBC12. The NEDD8-binding sequence in UBC4 identified on the basis of the present NMR data is poorly conserved in UBC12, which explains why UBC12 did not bind NEDD8 (**Supplementary Fig. 5** online). Obviously, ubiquitin and NEDD8 have distinct roles in the proteasome-dependent protein degradation system, despite the fact that these modifiers share 57% amino acid sequence identity. The present study suggests that once NEDD8 is attached onto the cullin subunit, it forms the active platform for selective recruitment of ubiquitin-charged E2 in collaboration with RBX1, excluding the UBC12–NEDD8 complex (**Supplementary Fig. 6** online), and thereby induces substrate ubiquitination. Indeed, cullin-1 neddylation enhances polyubiquitin chain elongation (**Fig. 2b,c**) as well as initial ubiquitin conjugation (**Supplementary Fig. 7** online). The E2-specific interaction of NEDD8 described here could be the mechanism that prevents poly-NEDD8 formation on cullins and concomitantly promotes polyubiquitination of substrates.

Note: Supplementary information is available on the Nature Structural & Molecular Biology website.

ACKNOWLEDGMENTS

We thank T. Kasuya, Y. Kito, K. Senda and K. Hattori for their help in the preparation of recombinant proteins. Work in the laboratory of K.K. and Y.Y. was supported by a Grant-in-Aid for Scientific Research on Priority Areas (17028047 and 18076003) from the Ministry of Education, Culture, Sports, Science and Technology, Japan, and by a Grant-in-Aid for Scientific Research (B) (18390016) from Japan Society for the Promotion of Science. E.S. is a recipient of Japan Society for the Promotion of Science Research Fellowships for Young Scientists.

AUTHOR CONTRIBUTIONS

K.K. contributed to overall guidance of the project. E.S., Y.Y. and K.K. contributed to the design and execution of the NMR study. E.S., K.I., T.C. and K.T. contributed to the design of the mutational studies. E.S., Y.M., Y.S. and N.M. contributed to the execution of the mutational studies. E.S. and K.K. wrote the manuscript. K.I., T.C. and K.T. commented on the manuscript. All authors edited and approved the final version of the manuscript.

COMPETING INTERESTS STATEMENT

The authors declare that they have no competing financial interests.

Published online at http://www.nature.com/nsmb/
Reprints and permissions information is available online at http://npg.nature.com/reprintsandpermissions

1. Petroski, M.D. & Deshaies, R.J. *Nat. Rev. Mol. Cell Biol.* **6**, 9–20 (2005).
2. Kerscher, O., Felberbaum, R. & Hochstrasser, M. *Annu. Rev. Cell Dev. Biol.* **22**, 159–180 (2006).
3. Pan, Z.Q., Kentsis, A., Dias, D.C., Yamoah, K. & Wu, K. *Oncogene* **23**, 1985–1997 (2004).
4. Wu, J.T., Chan, Y.R. & Chien, C.T. *Trends Cell Biol.* **16**, 362–369 (2006).
5. Parry, G. & Estelle, M. *Semin. Cell Dev. Biol.* **15**, 221–229 (2004).
6. Wei, N. & Deng, X.W. *Annu. Rev. Cell Dev. Biol.* **19**, 261–286 (2003).
7. Kawakami, T. *et al. EMBO J.* **20**, 4003–4012 (2001).
8. Wu, K., Chen, A., Tan, P. & Pan, Z.Q. *J. Biol. Chem.* **277**, 516–527 (2002).
9. Zheng, N. *et al. Nature* **416**, 703–709 (2002).
10. Zheng, N., Wang, P., Jeffrey, P.D. & Pavletich, N.P. *Cell* **102**, 533–539 (2000).
11. Megumi, Y. *et al. Genes Cells* **10**, 679–691 (2005).

THE JOURNAL OF BIOLOGICAL CHEMISTRY VOL. 282, NO. 10, pp. 7137–7144, March 9, 2007

A Neural-specific F-box Protein Fbs1 Functions as a Chaperone Suppressing Glycoprotein Aggregation*

Received for publication, December 5, 2006 Published, JBC Papers in Press, January 10, 2007, DOI 10.1074/jbc.M611168200

Yukiko Yoshida[‡§1], **Arisa Murakami**[‡§], **Kazuhiro Iwai**[§¶], **and Keiji Tanaka**[‡]

From the [‡]*Tokyo Metropolitan Institute of Medical Science, 3-18-22 Honkomagome, Bunkyo-ku, Tokyo 113-8613,* [§]*CREST, Japan Science and Technology Corporation (JST), Saitama 332-0012, and the* [¶]*Department of Molecular Cell Biology, Graduate School of Medicine, Osaka City University, 1-4-3 Asahi-cyo, Abeno-ku, Osaka 545-8585, Japan*

Fbs1 is an F-box protein present abundantly in the nervous system. Similar to the ubiquitously expressed Fbs2, Fbs1 recognizes *N*-glycans at the innermost position as a signal for unfolded glycoproteins, probably in the endoplasmic reticulum-associated degradation pathway. Here, we show that the *in vivo* majority of Fbs1 is present as Fbs1-Skp1 heterodimers or Fbs1 monomers but not SCF^{Fbs1} complex. The inefficient SCF complex formation of Fbs1 and the restricted presence of SCF^{Fbs1} bound on the endoplasmic reticulum membrane were due to the short linker sequence between the F-box domain and the sugar-binding domain. *In vitro*, Fbs1 prevented the aggregation of the glycoprotein through the N-terminal unique sequence of Fbs1. Our results suggest that Fbs1 assists clearance of aberrant glycoproteins in neuronal cells by suppressing aggregates formation, independent of ubiquitin ligase activity, and thus functions as a unique chaperone for those proteins.

The SCF (Skp1/Cul1/F-box protein) complex, the largest known class of sophisticated E3[2] ubiquitin ligases, consists of common components, Skp1, Cul1, and Roc1/Rbx1, as well as variable components known as F-box proteins that bind the substrates (1, 2). In this complex, the scaffold protein Cul1 (alias cullin1) interacts at the N terminus with the adaptor subunit Skp1 and at the C terminus with the RING-finger protein Roc1/Rbx1 that recruits a specific ubiquitin-activating enzyme (E2) for ubiquitylation. F-box proteins, interacting with Skp1 through the ~40 amino acid F-box motif, play an indispensable role in the selection of target proteins for degradation because each distinct F-box protein usually binds a protein substrate(s) with a degree of selectivity for ubiquitylation through C-terminal protein-protein interaction domains (3). The human genome contains 69 genes for F-box proteins and a large number of F-box proteins function in the specific ubiquitylation of a wide range of substrates. The F-box proteins are divided into three classes according to the type of substrate-binding domains. The two classes of binding domains are WD40 repeats and leucine-rich repeats, which are named Fbw (or FBXW) and Fbl (or FBXL) families, respectively (4). The third class of F-box proteins is the Fbx (or FBXO) family that does not contain any of these domains.

It has been reported that a subfamily under the Fbx family consists of at least five homologous F-box proteins containing a conserved FBA motif (5, 6). Among them, Fbs1/Fbx2/NFB42/Fbg1 and Fbs2/Fbx6b/Fbg2 can bind to proteins with high mannose oligosaccharides modification that occurs in the endoplasmic reticulum (ER) (7). Experiments using a fully reconstituted system showed that both Fbs1 and Fbs2 can form SCF-type ubiquitin ligase complexes specific for *N*-linked glycoproteins (7, 8). Overexpression of the Fbs1 or Fbs2 dominant-negative form or decrease of endogenous Fbs2 by small interfering RNA resulted in inhibition of degradation of endoplasmic reticulum-associated degradation (ERAD) substrates, suggesting the involvement of SCF^{Fbs1} and SCF^{Fbs2} in the ERAD pathway. Interestingly, x-ray crystallographic and NMR studies of the substrate-binding domain of Fbs1 have revealed that Fbs1 interacts with the innermost chitobiose in *N*-glycans of glycoproteins by a small hydrophobic pocket located at the top of the β-sandwich, indicating that both Fbs1 and Fbs2 efficiently recognize the inner chitobiose structure in $Man_{3-9}GlcNAc_2$ glycans (9). Indeed, the introduction of point mutation into the residues in the pocket impaired the binding activity toward its glycoprotein substrates. In general, the internal chitobiose structure of *N*-glycans in many native glycoproteins is not accessible by macromolecules. Fbs1 interacted with denatured glycoproteins more efficiently than native proteins, indicating that the innermost position of *N*-glycans becomes exposed upon protein denaturation and used as a signal of unfolded glycoproteins to be recognized by Fbs1 (10).

Of the Fbs family proteins, whereas Fbs2 is distributed ubiquitously in a variety of cells and tissues, Fbs1 is expressed only in neurons (7). In considering the involvement of these F-box proteins in the ERAD pathway in general, the restricted expression of Fbs1 in neurons remains a mystery. In this study, we found that the major population of Fbs1 protein did not form the SCF^{Fbs1} complex in cells although Fbs1 is known to act as a compartment of SCF-type ubiquitin ligase (8). Moreover, the results showed that the sequence of the intervening segment between the F-box domain and the substrate-binding domain of the Fbs1 hampered the assembly of the SCF^{Fbs1} complex in the cytosol without affecting the association with Skp1. The Skp1-Fbs1 heterodimers as well as SCF^{Fbs1} complex effectively prevented the aggregation of the glycoprotein *in vitro*, and this

* This work was supported by grants from the Ministry of Education Science and Culture of Japan (to Y. Y. and K. T.). The costs of publication of this article were defrayed in part by the payment of page charges. This article must therefore be hereby marked "*advertisement*" in accordance with 18 U.S.C. Section 1734 solely to indicate this fact.

[1] To whom correspondence should be addressed. Tel.: 81-3-3823-2105; Fax: 81-3-3823-2965; E-mail: yyosida@rinshoken.or.jp.

[2] The abbreviations used are: E3, ubiquitin ligase; ER, endoplasmic reticulum; ERAD, ER-associated degradation; TBS, Tris-buffered saline; RNaseB, ribonuclease B; HA, hemagglutinin.

activity was dependent on the presence of the N-terminal domain and the substrate-binding domain of Fbs1. Our data thus imply that Skp1 and Fbs1 may function in both SCF and non-SCF complexes.

EXPERIMENTAL PROCEDURES

Affinity Purification and Immunoprecipitation of Brain Lysate—The preparation of lysates from mouse brains and purification of Fbs1 by using a ribonuclease B (RNaseB) column were performed as described previously (10). For immunoprecipitation, we used polyclonal antibody to Fbs1 as described previously (11). For immunoblotting, we used rabbit polyclonal antibodies against Fbs1, Cul1 (Zymed Laboratories Inc., San Francisco, CA) and Skp1 (Santa Cruz Biotechnology, Santa Cruz, CA), and horseradish peroxidase-conjugated goat anti-rabbit IgG (Jackson ImmunoResearch Laboratories, West Grove, PA) for Fbs1 and Skp1 blots or horseradish peroxidase-conjugated goat anti-rabbit IgG light chain (Jackson ImmunoResearch Laboratories) for Cul1 blots. Lectin blotting was performed by using horseradish peroxidase-conjugated ConA (Seikagaku-kogyo, Japan) as described previously (11).

Glycerol Gradient Analysis—The fraction eluated with 0.1 M chitobiose from the RNaseB resin was prepared from 0.5 ml of lysates (14 mg/ml) from mouse brains. The eluate was dialyzed against TBS. The resultant fraction and a 1-mg lysate of brains were used for glycerol gradient analysis. Samples and molecular weight markers (Amersham Biosciences) were fractionated by 4–17% (v/v) linear glycerol density gradient centrifugation (22 h, 100,000 × *g*) as described previously (12).

Cell Culture and Immunological Analysis—PC12 cells were grown in RPMI medium 1640 (Invitrogen) supplemented with 10% horse serum and 5% fetal bovine serum. For neuronal differentiation, PC12 cells were treated with 10–20 ng/ml nerve growth factor (Invitrogen) on collagen-coated plates. 293T and HeLa cells were grown in Dulbecco's modified Eagle's medium (Sigma) supplemented with 10% fetal bovine serum and were transfected as described previously (8). FLAG-tagged Fbs1 mutant vectors consisting of Fbs1 and Fbs2 fragments were generated by PCR, and those sequences were verified. Whole cell lysates were prepared with 20 mM Tris-HCl (pH 7.5), 150 mM NaCl (TBS) containing 0.5% Nonidet P-40. The supernatant and precipitate fractions were prepared by ultracentrifugation of the supernatant that was prepared by centrifugation of freezing-and-thawing cell lysates in TBS at 8,000 × *g* for 20 min and at 100,000 × *g* for 60 min. The precipitate fraction was solubilized with Triton X-100. Each immunoprecipitation analysis was performed for whole cell lysates or subcellular fraction of cells by using the same amount of proteins. Monoclonal antibodies to calnexin and rhodopsin were purchased from BD Transduction Laboratories and Affinity Bioreagents (Golden, CO), respectively. Antibodies to FLAG, HA, and fetuin have been described previously (8).

Pulse-chase Analysis—The expression plasmid for P23H rhodopsin was kindly provided by M. E. Cheetham (University College London). Pulse-chase experiments were performed as described previously (7). Briefly, 293T cells were transfected with 1 μg of P23H rhodopsin expression plasmid and 1 μg of FLAG-tagged Fbs1 derivatives or pcDNA3-FLAG plasmid. Twenty-four hours after transfection, the cells were starved for 30 min and labeled for 1 h with 150 μCi of Pro-Mix L-^{35}S *in vitro* cell labeling mix (Amersham Biosciences) per milliliter. After washing, the cells were chased with complete Dulbecco's modified Eagle's medium supplemented with fetal bovine serum in the presence or in the absence of 50 μg/ml MG132 (Peptide Institute, Tokyo, Japan) for the indicated time intervals. After the harvested cells were lysed by TBS containing 0.1% SDS and 1% Nonidet P-40, immunoprecipitation was performed with anti-rhodopsin and FLAG antibodies.

Preparation of Recombinant Proteins and in Vitro Ubiquitylation Assay—The His-tagged Fbs1 ΔF, Fbs1 ΔP baculovirus were produced by Bac-to-Bac baculovirus expression system (Invitrogen). The SCF^{Fbs1}, Skp1-Fbs1 dimers, Fbs1 Fbs1 ΔF, Fbs1 ΔP, Skp1-ΔP dimers, and Fbs1 ΔN were obtained by baculovirus-infected HighFive cells as described previously (10). These proteins were purified by affinity chromatography using RNaseB-immobilized beads as a ligand and chitobiose as an eluent, and the eluates were dialyzed to 1,000 volumes of TBS three times. *In vitro* ubiquitylation assays were performed as described previously (10).

Aggregation Assay—Jack bean α-mannosidase (Sigma) was desalted using a NAP-25 gel filtration column (Amersham Biosciences) equilibrated in 10 mM Tris-HCl (pH 8.0). The desalted protein was lyophilized and redissolved at 21.7 μM in 0.1 M Tris-HCl (pH 8.0) and 6 M GdnHCl as described previously (13). After denaturation for 60 min at room temperature, samples were diluted to 0.3 μM in 1 ml of TBS containing various concentrations of bovine serum albumin or recombinant Fbs1 derivatives. Protein aggregation was monitored at 25 °C over a period of 60 min by measuring absorbance at 360 nm.

RESULTS

Multiple States of Fbs1 in Brain—Fbs1 has been found in the fraction eluted with di-*N*-acetyl-D-glucosamine (thereafter referred to as chitobiose) from GlcNAc-terminated fetuin of lysates prepared from mouse brain (8). Fbs1 and Skp1 proteins were detected in the eluted fraction with Coomassie Brilliant Blue staining, but we could not detect the apparent band of Cul1. However, the formation of the SCF^{Fbs1} complex was confirmed not only by reciprocal immunoprecipitation experiments in 293T cells but also by reconstitution of baculovirally expressed recombinant SCF^{Fbs1} proteins. To address these contradictory observations, we tested whether endogenous Fbs1 in the mouse brain forms the SCF complex by examining the interaction of Fbs1 with Cul1 (Fig. 1*A*). Fbs1 can be easily purified by affinity chromatography using RNaseB that contains a high mannose oligosaccharide as a ligand and chitobiose as an eluent (10). Since Fbs1 contains a single binding domain toward an *N*-glycan, it seems likely that the eluated Fbs1 protein or its complex from the RNaseB-immobilized resin is free from its substrates. Indeed, the glycoproteins modified with high mannose oligosaccharides were not included in the eluates by chitobiose (Fig. 1*B*). Although Skp1 was effectively co-immunoprecipitated with Fbs1 from the lysate of mouse brain, the amount of Skp1 that was eluted with Fbs1 from the RNaseB resin was small (Fig. 1*A*). Despite the difference in the quantities of Skp1 bound to Fbs1 in the fractions between eluates from

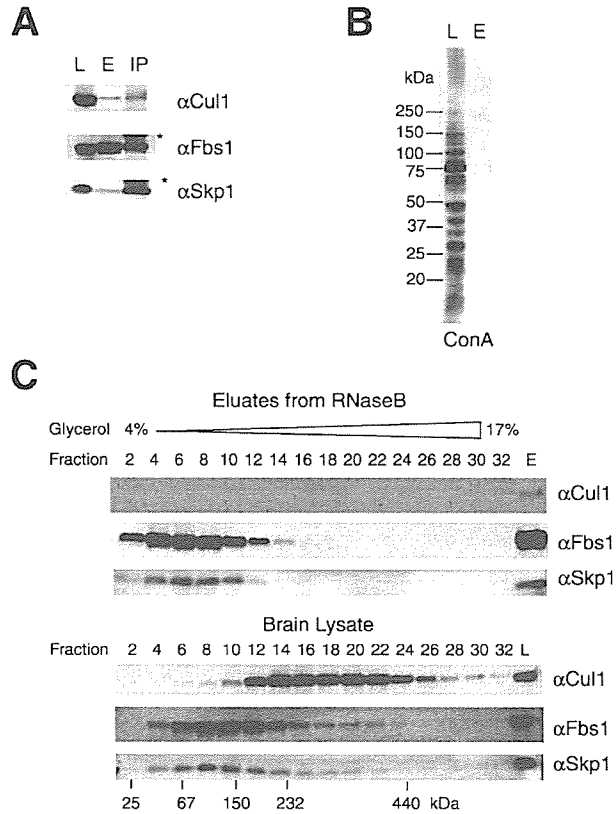

FIGURE 1. **States of Fbs1 in mouse brain.** *A*, 0.6 mg of lysate from adult mouse brain was subjected to RNaseB-immobilized affinity column and eluated with chitobiose (*E*) or subjected to immunoprecipitation with an antibody to Fbs1 (*IP*). Thirty μg of lysate (*L*), one-tenth of eluate, and immunoprecipitate were analyzed by immunoblotting with antibodies to Cul1, Fbs1, or Skp1. *Asterisks* show Ig heavy chain (*αFbs1*) and light chain (*αSkp1*). *B*, ConA lectin blot for brain lysate (*L*) and the eluate from the RNaseB resin (*E*) against the same amounts of proteins described in *A*. *C*, adult mouse brain lysate (*lower panel*, 0.7 mg) and lysate eluated with chitobiose from RNaseB (*upper panel*, started from 7 mg of the lysate) were separated by 4–17% glycerol density gradient centrifugation. One-third of each fraction was analyzed by immunoblotting with antibodies to Cul1, Fbs1, and Skp1. *Molecular size markers* are indicated below.

the RNaseB resin and immunoprecipitation with an anti-Fbs1 antibody, almost the same and small quantities of Cul1 were detected in these fractions. These results suggest that major populations of substrate-free Fbs1 and substrate-binding Fbs1 are present as Fbs1 monomers and Fbs1-Skp1 dimers, respectively, and the binding of substrates to Fbs1 does not influence the weak SCF complex formation.

To examine the behavior of endogenous Fbs1 in more detail, eluates from the RNaseB resin and lysates from the mouse brain were separated by a 4–17% glycerol density gradient centrifugation (Fig. 1*C*). The distribution of Fbs1 (~42 kDa) in the chitobiose eluates corresponded to the position of Fbs1 monomers (fraction 4) and Skp1-Fbs1 dimers (~63 kDa)(fraction 6). Although Cul1 was not detected in any fractions, the peak of Skp1 in eluates from the RNaseB resin was in the position of the Skp1-Fbs1 dimer. On the other hand, Fbs1 protein in brain lysate was detected in a broad range of fractions mainly larger than Fbs1-Skp1 dimers, indicating that most Fbs1, if not all, is associated with various glycoprotein substrates; *i.e.* Fbs1-Skp1 dimers maintain the association with glycoproteins *in vivo*. Cul1 (~90 kDa) in brain lysate was distributed broadly in higher density fractions, indicating its association with various other SCF-components.

Minor Population of Fbs1 Forms SCF Complex on ER—We next expressed FLAG-tagged F-box proteins alone or their combination with HA-tagged Skp1 in 293T cells and immunoprecipitated with anti-FLAG and anti-HA antibodies (Fig. 2*A*). The expression of HA-tagged Skp1 increased the amount of exogenous F-box proteins, suggesting that Skp1 stabilizes F-box proteins (*lanes 1–8*). Cul1 was co-immunoprecipitated with Fbs2 and Fbg3, which are highly homologous with Fbs1, or βTrCP1/Fbw1, one of the Fbw family members (*lanes 11–16*). The interaction between Cul1 and these F-box proteins increased upon co-expression of Skp1. However, unlike these F-box proteins, Fbs1 was almost undetectable in the immune complex with Cul1, regardless of the overexpression of exogenous Skp1 (*lanes 9* and *10*), although Fbs1 was co-immunoprecipitated with Skp1 as well as other F-box proteins (*lanes 18, 20, 22,* and *24* in the *αFlag panel*). Moreover, the amount of Cul1 associated with exogenous Skp1 was lower in the presence of Fbs1 than in those of other F-box proteins, suggesting that expression of Fbs1 prevents forming other SCF complexes by dimerizing with Skp1 (*lanes 18, 20, 22,* and *24* in the *αCul1 panel*). These results suggest that Fbs1 can strongly bind Skp1 but is weak in forming the SCF^{Fbs1} complex.

We have recently reported that Fbs1 is a cytosolic protein but that part of Fbs1 associates with the ER membrane through interaction with p97/VCP (valosin-containing protein) (11). We next examined whether the ER membrane-associated Fbs1 formed the SCF complex. Lysates of 293T and HeLa cells expressing FLAG-tagged Fbs1 were fractionated into the 100,000 × *g* supernatant and precipitate fractions excluding the 8,000 × *g* precipitate, and then Fbs1 was immunoprecipitated from these fractions by anti-FLAG antibody. As shown in Fig. 2*B*, Cul1 was co-immunoprecipitated with Fbs1 mainly from the precipitate (*p*) fraction (*lanes 4* and *8*). Although the association of Fbs1 with Skp1 occurred more effectively in the supernatant (*s*) fraction, the formation of the SCF complex, including Fbs1, was hardly detected in the supernatant fraction (*lanes 3* and *7*). Moreover, we examined whether endogenous Fbs1 formed the SCF complex in the precipitate fraction using nerve growth factor-treated PC12 cells, which endogenously express Fbs1 (14). As shown in Fig. 2*C*, part of Cul1 was co-immunoprecipitated with Fbs1 from the precipitate (*p*) fraction. These results indicate that the major population of endogenous Fbs1 is present as the Fbs1-Skp1 heterodimers or the Fbs1 monomers in the cytosol, and a minor population of Fbs1 forms the SCF complex bound on the ER membrane.

Linker Sequence of Fbs1 Prevents SCF Complex Formation—Although the SCF complex formation of Fbs1 was inefficient, Fbs2 formed the SCF complex effectively (Fig. 2*A*). To identify the region(s) of Fbs1 that impedes SCF complex formation, we examined the ability of various fusion proteins containing Fbs1 and Fbs2 fragments to form the complex and compared these findings with the full-length proteins in co-immunoprecipitation assay (Fig. 3*A*). Fbs1 ΔF was used as negative control that did not bind to Skp1 (Fig. 3*B*, *lane 3*). Fbs1 YW and Fbs1 ΔC, both of which are deficient in substrate binding, could not restore SCF complex formation, indicating that the interaction

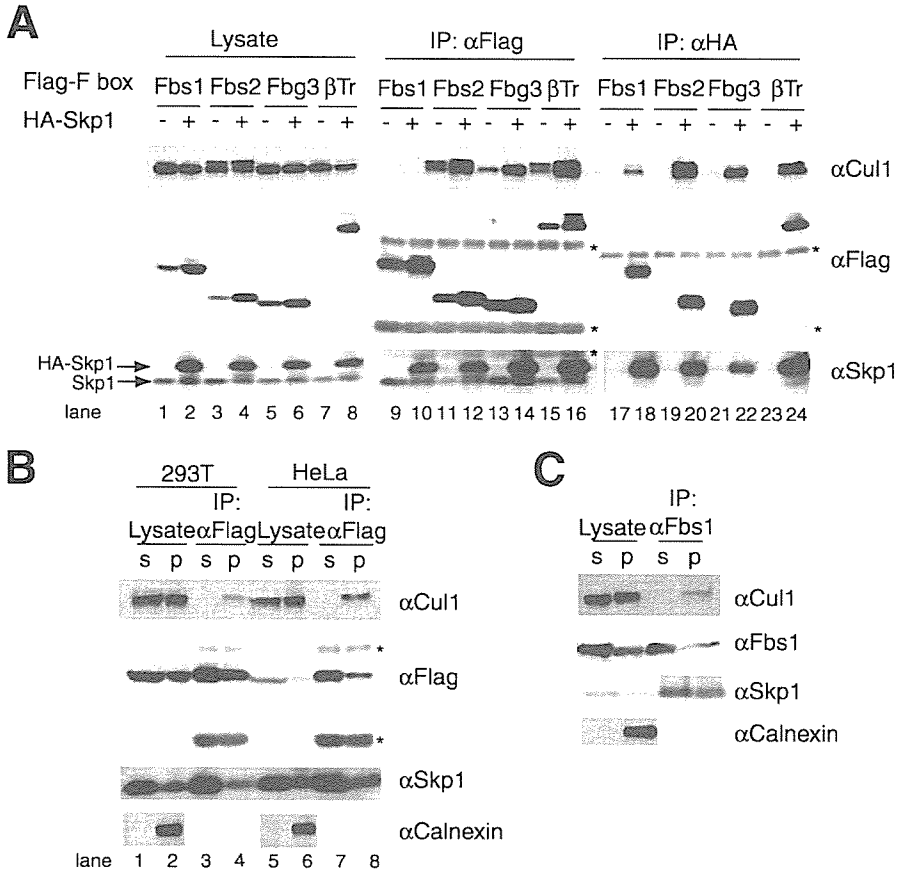

FIGURE 2. **Major population of Fbs1 forms non-SCF complex *in vivo*.** *A*, 293T cells were transfected with plasmids encoding various FLAG-tagged F-box proteins (Fbs1, Fbs2, Fbg3, and βTrCP1 (*βTr*)) combination with empty HA plasmids (−) or plasmids encoding HA-tagged Skp1 (+). Whole cell lysates were subjected to immunoprecipitation (*IP*) with antibodies to FLAG and HA, and lysates (15 μg each) and one half of the resulting precipitates were analyzed by immunoblotting with antibodies to Cul1, FLAG, and Skp1. *Asterisks* show Ig heavy and light chains. *B*, 293T and HeLa cells were transfected with FLAG-tagged Fbs1. Cell lysates were fractionated by ultracentrifugation, and FLAG-Fbs1 was immunoprecipitated with an antibody to FLAG from the same amount of proteins of 100,000 × *g* supernatant (*s*) and precipitate (*p*) fractions. The total amount of protein of the supernatant fraction was 2–3 times larger than that of the precipitate fraction. Lysates (15 μg each) and immunoprecipitates were analyzed by immunoblotting with antibodies to Cul1, FLAG, and Skp1. *Asterisks* show Ig heavy and light chains. To control for the fractionation, immunoblotting with an antibody to calnexin was performed. *C*, endogenous Fbs1 was immunoprecipitated with an antibody to Fbs1 from 100,000 × *g* supernatant, and precipitate fractions of differentiated PC12 cells were treated with nerve growth factor. Lysates (15 μg each) and immunoprecipitates were analyzed by immunoblotting. The immunoblotting analysis for separated supernatant and precipitate fractions was conducted as for *B*.

between Fbs1 and its substrates does not affect the complex formation (*lanes 4* and *5*). The N-terminal sequence of Fbs1 called the P domain is unique and is not seen in other F-box proteins, but the removal of this domain from Fbs1 or the addition to Fbs2 did not affect the complex formation (Fbs1 ΔP and Fbs2 P1: *lanes 6* and *13*). Exchange of the F-box domains between Fbs1 and Fbs2 caused the loss of the Skp1 binding activity, probably due to the incorrect folding (Fbs1 F2, Fbs1 ΔPF2, Fbs2 F1, and Fbs2 PF1: *lanes 7*, *8*, *10*, and *11*, respectively). However, the replacement of the Fbs1 N-terminal region (which contains P and F-box domains and linker sequence) with the Fbs2 N-terminal region rescued the complex formation (Fbs-2N1C: *lane 9*). In contrast, the addition of the Fbs1 N-terminal region instead of the Fbs2 N-terminal region markedly reduced the activity of Fbs2 to form the SCF complex but did not affect the Skp1 binding (Fbs-1N2C: *lane 12*). The linker sequences of the intervening segments between the F-box domain and the substrate-binding domain showed lower homology than other portions between Fbs1 and Fbs2, suggesting that the Fbs1 linker sequence is responsible for impeding the SCF^{Fbs1} complex formation. Indeed, only the Fbs1 mutant protein that contained the Fbs2 linker sequence could form the SCF complex, but the efficiency of the SCF complex formation was less than that of Fbs-2N1C (Fbs1 I2: *lane 15*). On the other hand, Fbs2 protein containing the Fbs1 linker sequence and the Fbs1 protein without its linker sequence did not seem to show the correct folding for Skp1 binding (Fbs2 I1 and Fbs1 ΔI: *lanes 16* and *17*). The Fbs1 mutant in which the F-box domain and the linker sequence are replaced with those of Fbs2 forms the SCF complex effectively. Thus, we conclude that the Fbs1 linker sequence between the F-box and substrate-binding domains hampers the SCF^{Fbs1} complex formation.

We next compared the localization of Fbs1, Fbs2, and the mutant Fbs1 proteins capable of forming the SCF complex: Fbs-2N1C and Fbs1 I2 (Fig. 3*C*). Although a minor population of Fbs1 in the precipitate (*p*) fraction formed the SCF complex, most Fbs2 formed the SCF^{Fbs2} complex in the supernatant (*s*) fraction as well as the precipitate fraction. Fbs-2N1C could form the SCF complex mainly in the supernatant fraction (Fig. 3*C*). Moreover, the amount of Cul1 co-immunoprecipitated with Fbs1 I2 was similar in both fractions. These results suggest that the linker sequence of Fbs1 does not only impede the formation of the SCF complex but also restricts the localization of the SCF complex bound on the ER membrane.

Expression of Mutant Fbs1 That Forms E3 Easily Induces Proteolysis of Its Substrates—To confirm that most Fbs1 in the cells is inactive to function as an E3 ubiquitin ligase, we next examined the ability of the mutant Fbs1 that readily forms the SCF complex (Fbs-2N1C) to ubiquitylate the substrates. It has been shown that P23H mutated rhodopsin (hereafter referred to as P23H) is an ERAD substrate, and its *N*-linked glycosylation is required for the degradation (15, 16). As reported previously, rhodopsin monomer is ~40–43 kDa, but the majority of P23H was detected as high molecular weight complex multimers by immunoblotting with anti-rhodopsin antibody (Fig. 4*A*). Wild-type Fbs1, but not the substrate-binding defective mutant Fbs1 YW, was able to associate with P23H effectively, suggesting that Fbs1 binds to P23H through its *N*-glycans. On the other hand,

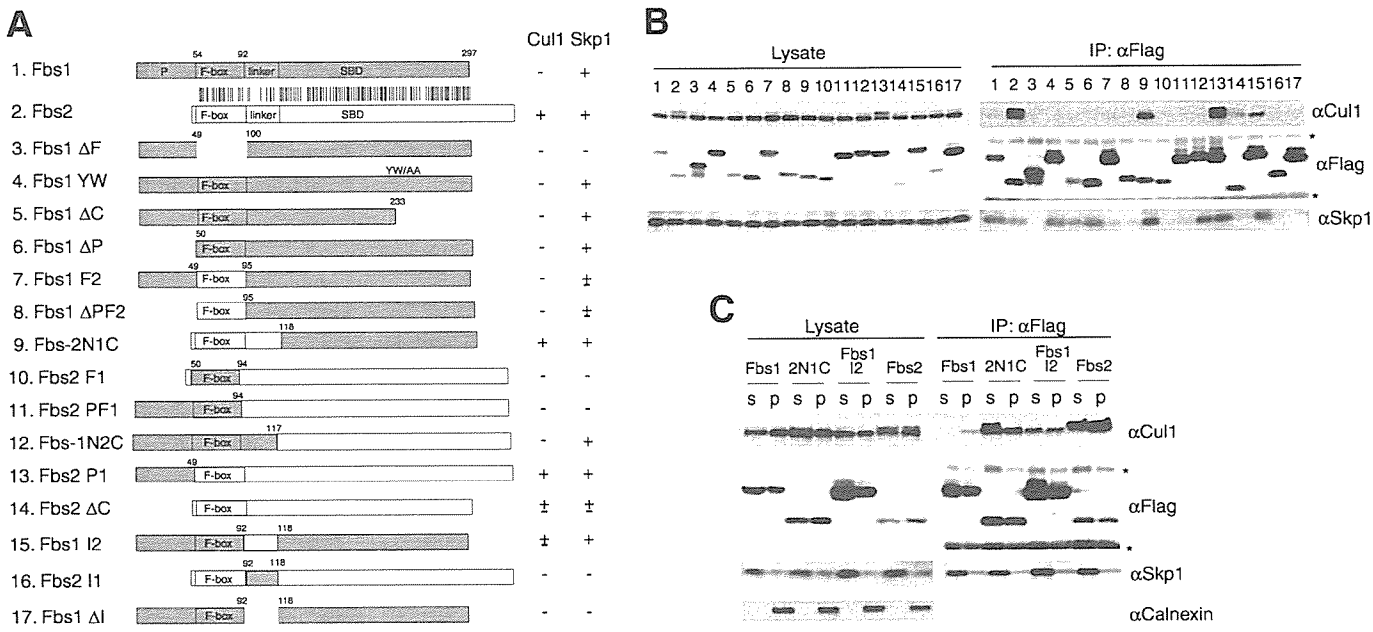

FIGURE 3. **Linker sequence between F-box and substrate-binding domains of Fbs1 hampers SCF^{Fbs1} complex formation.** *A*, schematic representation of constructs of fusion proteins consisting of Fbs1 and Fbs2 fragments. The fragments derived from Fbs1 and Fbs2 appear in *gray* and *white boxes*, respectively. The *numbers* above the constructs represent the amino acid position of Fbs1. The *vertical bars* represent identical amino acids between Fbs1 and Fbs2. P and F-box domains, linker sequence, and sugar-binding domain are represented by *P*, *F-box*, *linker*, and *SBD*, respectively. The binding activities of these constructs toward Cul1 and Skp1 shown in *B* are summarized on the *right*, with + representing strong binding, + representing weak binding, and − representing no binding. *B*, 293T cells were transfected with plasmids encoding the FLAG-tagged mutants F-box proteins represented in *A*. Whole cell lysates were subjected to immunoprecipitation (*IP*) with an antibody to FLAG, and the resulting precipitates were analyzed by immunoblotting with antibodies to Cul1, Skp1, and FLAG. *Asterisks* show Ig heavy and light chains. *C*, 293T cells were transfected with FLAG-tagged Fbs1, Fbs-2N1C, Fbs1 I2, or Fbs2. Cell lysates were fractionated by ultracentrifugation, and FLAG-Fbs1 was immunoprecipitated with an antibody to FLAG from 100,000 × *g* supernatant (*s*) and precipitate (*p*) fractions. The resulting immunoprecipitates were analyzed by immunoblotting as in Fig. 2*B*.

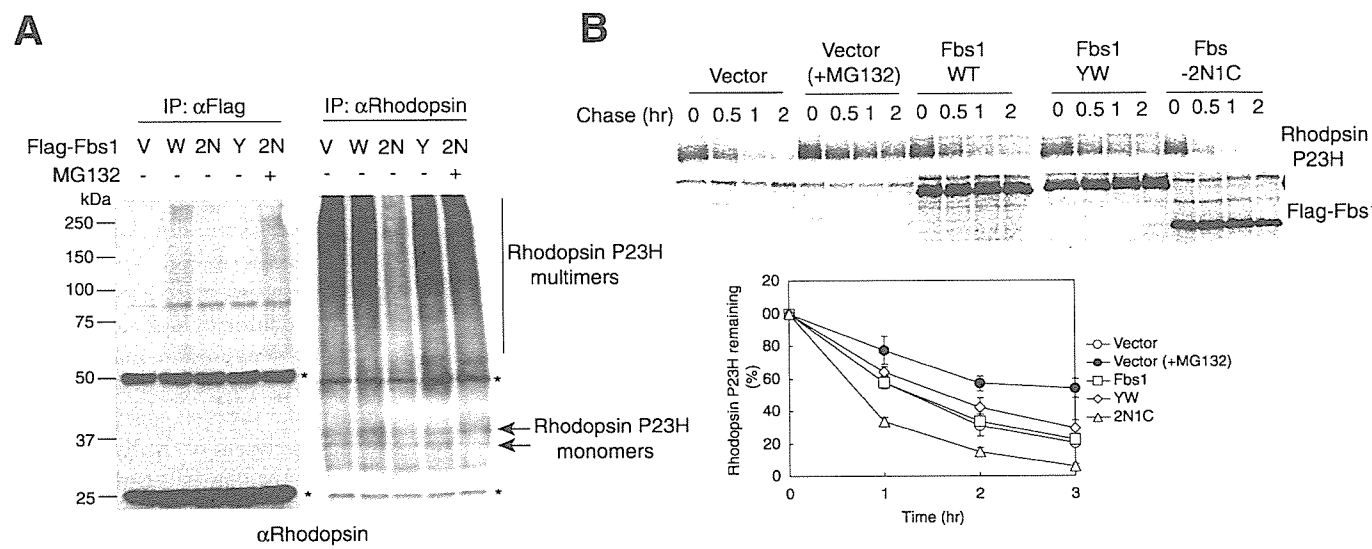

FIGURE 4. **Expression of Fbs-2N1C promotes substrate degradation.** *A*, 293T cells were transfected with plasmids encoding FLAG-tagged empty vector (*V*), Fbs1 (*W*), Fbs-2N1C (*2N*), or Fbs1 YW (*Y*) and combination with rhodopsin P23H mutant. Some cells were treated with 10 μM MG132 for 16 h. Whole cell lysates were subjected to immunoprecipitation (*IP*) with antibodies to FLAG and rhodopsin, and the resulting precipitates were analyzed by immunoblotting with an antibody to rhodopsin. *Asterisks* show Ig heavy and light chains. *B*, rhodopsin P23H was co-transfected with FLAG-tagged empty vector, Fbs1, Fbs-2N1C, or Fbs1 YW. Twenty-four hours after transfection, 293T cells were pulse-labeled with [^{35}S]Met/Cys for 1 h and chased for the indicated time intervals. Rhodopsin P23H and Fbs1 derivatives were immunoprecipitated with antibodies to rhodopsin and FLAG, respectively. The plotted data at the bottom show a quantification analysis of the stability of rhodopsin P23H over time in the *upper panels*. Data are the mean ± S.D. of three independent experiments. *WT*, wild type.

Fbs-2N1C could bind to P23H, although its binding to P23H seemed weaker than that of wild-type Fbs1 (Fig. 4*A*, *left panel*). Since the activity to bind RNaseB was not different between Fbs1 and Fbs-2N1C (data not shown), it seems likely that the $SCF^{Fbs\text{-}2N1C}$ causes degradation of P23H through its ubiquitylation. Interestingly, the quantity of P23H decreased upon Fbs-2N1C expression (Fig. 4*A*, *right panel*). It has been reported that the degradation of P23H was suppressed by MG132 treatment (15, 16). The quantities of both P23H associated with Fbs-2N1C and the P23H protein were recovered by the addition of MG132. Moreover, we performed pulse-chase analysis using 293T cells co-expressing the P23H mutant and FLAG-tagged